



**HAL**  
open science

## **Green tea infusion prevents diabetic nephropathy aggravation in recent-onset type 1 diabetes regardless of glycemic control**

Luiz Carlos Maia Ladeira, Eliziária Cardoso dos Santos, Talita Amorim Santos, Janaina da Silva, Graziela Domingues de Almeida Lima, Mariana Machado-Neves, Renê Chagas da Silva, Mariella Bontempo Freitas, Izabel Regina dos Santos Costa Maldonado

### ► **To cite this version:**

Luiz Carlos Maia Ladeira, Eliziária Cardoso dos Santos, Talita Amorim Santos, Janaina da Silva, Graziela Domingues de Almeida Lima, et al.. Green tea infusion prevents diabetic nephropathy aggravation in recent-onset type 1 diabetes regardless of glycemic control. *Journal of Ethnopharmacology*, 2021, 274, pp.114032. 10.1016/j.jep.2021.114032 . hal-03229076

**HAL Id: hal-03229076**

**<https://hal.science/hal-03229076>**

Submitted on 31 May 2021

**HAL** is a multi-disciplinary open access archive for the deposit and dissemination of scientific research documents, whether they are published or not. The documents may come from teaching and research institutions in France or abroad, or from public or private research centers.

L'archive ouverte pluridisciplinaire **HAL**, est destinée au dépôt et à la diffusion de documents scientifiques de niveau recherche, publiés ou non, émanant des établissements d'enseignement et de recherche français ou étrangers, des laboratoires publics ou privés.

1 **Green tea infusion prevents diabetic nephropathy's aggravation in recent-onset**  
2 **type 1 diabetes regardless of glycemetic control**

3 Running title: Tea and diabetic nephropathy

4 Luiz Carlos Maia Ladeira<sup>a\*</sup>, Eliziária Cardoso dos Santos<sup>b</sup>, Talita Amorim Santos<sup>a</sup>, Janaina da  
5 Silva<sup>a,c</sup>, Graziela Domingues de Almeida Lima<sup>a</sup>, Mariana Machado-Neves<sup>a</sup>, Renê Chagas da Silva<sup>d</sup>,  
6 Mariella Bontempo Freitas<sup>e</sup>, Izabel Regina dos Santos Costa Maldonado<sup>a</sup>.

7 <sup>a</sup> Departamento de Biologia Geral, Universidade Federal de Viçosa, Viçosa, Minas Gerais, Brasil.

8 <sup>b</sup> Escola de Medicina da Universidade Federal do Vale do Jequitinhonha e Mucuri, Diamantina,  
9 Minas Gerais, Brasil.

10 <sup>c</sup> Institut de Recherche en Santé, Environnement et Travail, Université de Rennes, Rennes, France.

11 <sup>d</sup> Departamento de Física, Universidade Federal de Viçosa, Viçosa, Minas Gerais, Brasil.

12 <sup>e</sup> Departamento de Biologia Animal, Universidade Federal de Viçosa, Minas Gerais, Brasil.

14  
15 ORCID-ID and e-mail:

16 Luiz Carlos Maia Ladeira - 0000-0002-7152-2688 – [luizmaialadeira@gmail.com](mailto:luizmaialadeira@gmail.com)

17 Eliziária Cardoso dos Santos - 0000-0002-3030-7746 – [lisa.famed@gmail.com](mailto:lisa.famed@gmail.com)

18 Talita Amorim Santos - 0000-0003-3242-7554 - [taliamorims@gmail.com](mailto:taliamorims@gmail.com)

19 Janaina da Silva - 0000-0002-8782-1148 - [janaina.silva2@ufv.br](mailto:janaina.silva2@ufv.br)

20 Graziela Domingues de Almeida Lima – 0000-0001-5954-3606 - [graziela.gdal@gmail.com](mailto:graziela.gdal@gmail.com)

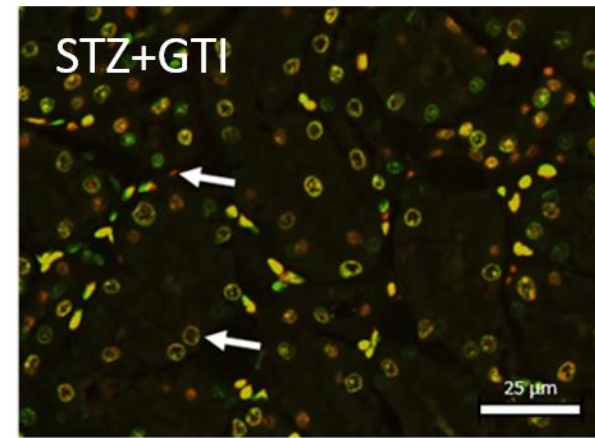
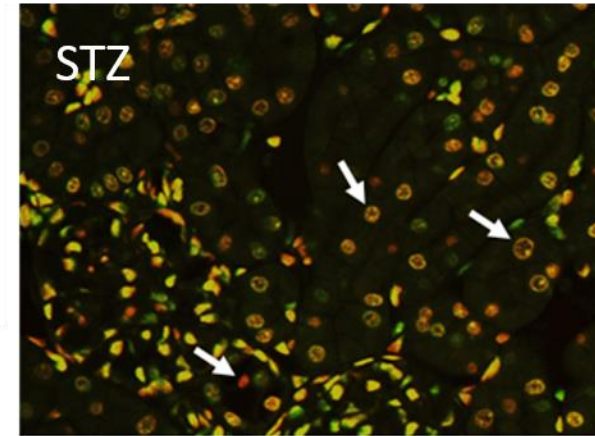
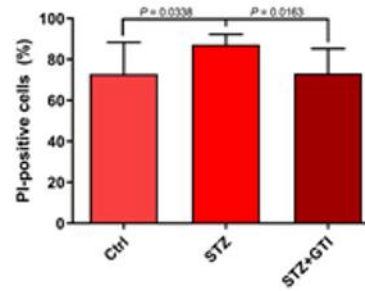
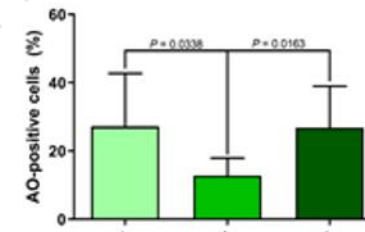
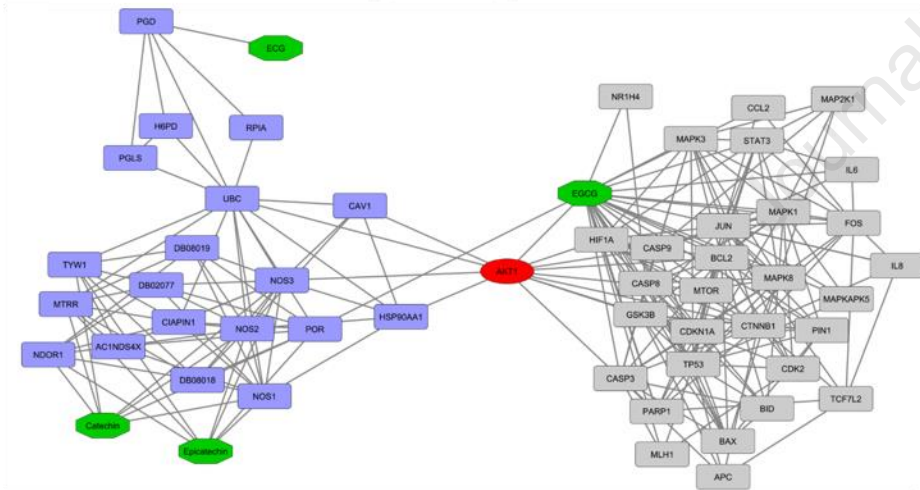
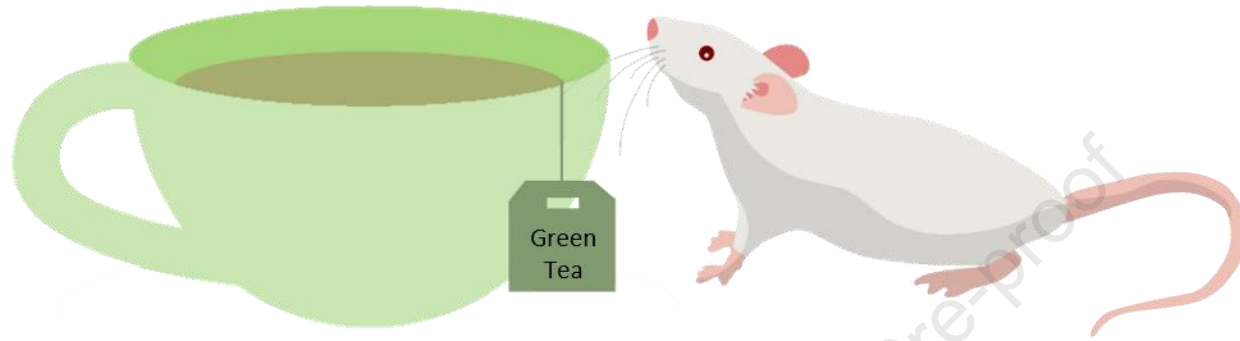
21 Mariana Machado-Neves – 0000-0002-7416-3529 - [machadonevesm@gmail.com](mailto:machadonevesm@gmail.com)

22 Renê Chagas da Silva - 0000-0002-8073-325X – [rene.silva@ufv.br](mailto:rene.silva@ufv.br)

23 Mariella Bontempo Freitas - 0000-0001-5132-242X - [mariellafreitas@gmail.com](mailto:mariellafreitas@gmail.com)

24 Izabel Regina dos Santos Costa Maldonado - 0000-0003-3884-253X – [irscmaldonado@gmail.com](mailto:irscmaldonado@gmail.com)

26  
27  
28 **\*Corresponding author:** Departamento de Biologia Geral, Universidade Federal de Viçosa. Av.  
29 P.H. Rolfs, s/n, Campus Universitário, Viçosa 36570-900, Minas Gerais, Brasil. Phone: +55 (31)  
30 3612-2515. E-mail address: [luizmaialadeira@gmail.com](mailto:luizmaialadeira@gmail.com) (Ladeira, L. C. M.).



**34 Abstract**

35 Ethnopharmacological relevance: Green tea, traditionally used as antidiabetic medicine, affects  
36 positively the diabetic nephropathy and it was assumed that these beneficial effects were due to the  
37 tea's hypoglycemic capacity, reducing the glycemic overload and, consequently, the advanced  
38 glycation end products rate and oxidative damage. However, these results are still controversial  
39 because tea is not always able to exert a hypoglycemic action, as shown by previous studies.

40 Aim: Investigate if green tea infusion can generate positive outcomes for the kidney independently  
41 of glycemic control, using a model of severe type 1 diabetes.

42 Material and methods: We treated streptozotocin type 1 diabetic young rats with 100 mg/Kg of  
43 green tea, daily, for 42 days, and evaluated the serum and tissue markers for stress and function,  
44 also, we analyzed the ion dynamics in the organ and the morphological alterations promoted by  
45 diabetes and green tea treatment. Besides, we analyzed, by an *in silico* approach, the interactions of  
46 the green tea main catechins with the proteins expressed in the kidney.

47 Results: Our findings reveals that the components of green tea can interact with proteins  
48 participating in cell signaling pathways that regulate energy metabolism, including glucose and  
49 glycogen synthesis, glucose reabsorption, hypoxia management, and cell death by apoptosis. Such  
50 interaction leads to reduced accumulation of glycogen in the organ, as well as protects DNA. These  
51 results also reflect in a preserved glomerulus morphology, with improvement in pathological  
52 features, and suggesting a prevention of kidney function impairment.

53 Conclusion: Our results show that such benefits are achieved regardless of the blood glucose status,  
54 and are not dependent on the reduction of hyperglycemia.

55

**56 Keywords:**

57 Diabetic nephropathy; type 1 diabetes; recent-onset diabetes; diabetic kidney disease; green tea.

## 58 1. Introduction

59 Diabetic nephropathy (DN) affects 25% - 35% of type 1 and 2 diabetic patients (Herman-  
60 Edelstein and Doi, 2016), and account for about 45% of the patients with end-stage renal disease  
61 (Su et al., 2020). It progresses from the increase in the glomerular filtration rate to the total failure  
62 of the kidneys, passing through alterations that indicate damage to the renal glomeruli and tubules,  
63 albuminuria, mesangial expansion, fibrosis, and vascular damage (Gilbert, 2017; Herman-Edelstein  
64 and Doi, 2016). In addition, glycogenic accumulation in the proximal tubules is a common feature  
65 in DN, and one of the earliest signals of metabolic impairment in the organ (Gilbert, 2017;  
66 Haraguchi et al., 2020). Such damage can progress in renal cells to pre-neoplastic lesions which, if  
67 left untreated, may progress to renal cancer (Ribback et al., 2015).

68 Green tea (*Camellia sinensis* (L.) Kuntze (Theaceae)), popularly used as a traditional  
69 medicine, in the form of infusion, for many porpoises including hyperglycaemia (Barkaoui et al.,  
70 2017; Chopade et al., 2008; Fallah Huseini et al., 2006; Rachid et al., 2012), is known to exert  
71 positive effects in diabetes management (Meng et al., 2019; Mohabbulla Mohib et al., 2016).  
72 Recent studies have shed light on the mechanisms that tea catechins affect positively the DN, with  
73 special focus on the podocyte (Hayashi et al., 2020), through the activation of the 67kDa laminin  
74 receptor (67LR) by the epigallocatechin gallate (EGCG), the main polyphenol in green tea. Such  
75 interaction results in the preservation of podocyte morphology and the glomerular filtration  
76 function, suggesting an improvement in DN. However, tubular alterations, with glycogen  
77 accumulation, and aberrant activation of the advanced glycated end-products and its receptor  
78 (AGE/RAGE system), affecting the cellular renovation and survival, are seem to be the primary  
79 cause of proximal tubular function disruptment (Haraguchi et al., 2020). This, in turn, can affect  
80 glomerular function by the proximal tubule/glomerulus feedback system, leading to glomerular  
81 damage and contributing to the progression of DN.

82           It was assumed that the beneficial effects of the green tea on proximal tubules were due to  
83 the tea's hypoglycemic capacity (Renno et al., 2008; Yokozawa et al., 2012), reducing the  
84 glycemic overload and consequently AGE rate and oxidative damage. However, tea effects in  
85 diabetic human subjects are still controversial. The first double-blind controlled trial treating  
86 diabetic patients (being 100% type 2 diabetic) with green tea polyphenols describes a reduction in  
87 podocyte apoptosis and an improvement of kidney function by reducing microalbuminuria (Borges  
88 et al., 2016). Another double-blind controlled trial conducted with diabetic adult patients (being  
89 70.3% type 1 diabetic) fail to achieve glycemic control or improve renal function after green tea  
90 consumption (Vaz et al., 2018). On the other hand, tea catechins can inhibit gluconeogenesis by  
91 activating the 5'AMP-activated protein kinase (AMPK) (Collins et al., 2007), possibly reducing  
92 glycogenic nephrosis. Also, EGCG can activate the protein kinase B (AKT) pathway enhancing cell  
93 survival and preserving nephron morphology (Hayashi et al., 2020). These effects may contribute to  
94 the prevention of DN development in recent-onset diabetes (Haraguchi et al., 2020).

95           In a previous study, we demonstrated that the infusion of green tea was not able to prevent  
96 hyperglycemia in animals with experimental type 1 diabetes induced by streptozotocin (STZ) in  
97 young male Wistar rats (Ladeira et al., 2020a). Therefore, in the same model, we tested the  
98 hypothesis that the beneficial effects of tea in DN go beyond glycemic control. In this way, we  
99 investigated the effects of green tea infusion treatment on diabetic kidney disease in recent-onset  
100 type 1 diabetic young rats. Also, we used bioinformatics tools to explore tea catechin interaction in  
101 signaling pathways in the kidney.

102

## 103 2. Materials and methods

### 104 2.1. Animals and ethics

105 Eighteen male Wistar rats (30 days old;  $82.52 \pm 10.83\text{g}$ ) were housed, two per cage, in  
106 polypropylene cages with autoclaved sawdust as cage bed, under controlled conditions of  
107 temperature ( $22 \pm 2 \text{ }^\circ\text{C}$ ) and light-dark cycles (12/12h), and received food (Presença Alimentos,  
108 Paulínea, SP, Brazil) and water *ad libitum*. The use of animals in the research was approved by the  
109 Ethics Committee of Animal Use of the Federal University of Viçosa (CEUA/UFV – protocol  
110 number 53/2018).

111

### 112 2.2. Green tea infusion preparation and analysis

113 Green tea (*Camellia sinensis*) leaves were obtained from Leão<sup>®</sup> - Food and Beverages  
114 (Coca-Cola Company<sup>®</sup>, lot LO159), and prepared as infusion, to mimic the way it is normally  
115 consumed by humans. The infusion was prepared mixing the leaves with warm distilled water (1:40  
116 w/v,  $80 \text{ }^\circ\text{C}$ ) (Perva-Uzunalić et al., 2006). The mixture remained infused for 20 minutes on a  
117 magnetic stirrer. Then, it was filtered through a  $0.45 \text{ }\mu\text{m}$  porous filter, frozen at  $-80 \text{ }^\circ\text{C}$  and  
118 lyophilized. The lyophilized samples were resuspended in distilled water at the moment of use.

119 The chromatographic profile, or fingerprint, was determined as described by Kim-Park et al.  
120 (Kim-Park et al., 2016), with some modifications. High-performance liquid chromatography  
121 (HPLC) (Prominence LC-20A, Shimadzu, Kyoto, Japan), equipped with Diode Arrangement  
122 Detector (DAD), LC-20AD pump, SPD-M20A detector, CTO-20A oven and LabSolutions  
123 software, was used to determine the EGCG content using a maximal absorption peaks at 272nm. It  
124 was used a Vydac C18 (4.6 x 250 mm) column, at  $30 \text{ }^\circ\text{C}$ , with a  $5\mu\text{L}$  injection volume. The mobile  
125 phase was composed of water and 2.0% acetic acid (1:1). The infusion lyophilized powder was  
126 suspended in methanol before analysis. The mobile phase flow rate was 1.0 mL/min and the run

127 time was 15 min. The retention time of the main component, EGCG, was 4.5 min and the total  
128 amount of it was calculated using a standard curve ( $r^2 = 0.9967$ ) developed under the same  
129 conditions using an EGCG chemical standard ( $\geq 98.0\%$ , Sigma Aldrich Inc. - CAS Number 989-51-  
130 5. St. Louis, MO, USA). The EGCG content was shown to be 19.38% of the total GTI content. The  
131 fingerprint is presented in the Figure 1.

132 Also, we determined the total phenolic content and antioxidant capacity as previously  
133 described (Ladeira et al., 2020a). GTI presented a total amount of phenolic components of  $3.88 \pm$   
134  $2.49$  mg gallic acid equivalent (GAE)/g GTI. The extract presented an antioxidant capacity of  $3.26$   
135  $\pm 0.06$   $\mu\text{Mol}$  Trolox equivalent (TE)/g GTI in the 2,2'-Azinobis-[3-ethylbenzthiazoline-6-sulfonic  
136 acid] (ABTS) assay and  $46.38 \pm 4.10$   $\mu\text{Mol}$   $\text{FeSO}_4$ /g GTI in the ferric reducing antioxidant power  
137 (FRAP) assay.

138

139

### 140 2.3. Experimental design, euthanasia, and tissue collection

141 Twelve rats were randomly selected to integrate the diabetics groups. After 12h fasting, diabetes  
142 was induced by a single intraperitoneal (i.p.) injection of streptozotocin (STZ) (Sigma Chemical  
143 Co., St, Louis, MO, USA) at a dosage of 60 mg/kg of body weight (BW) diluted in 0.01 M sodium  
144 citrate buffer, pH 4.5. The healthy control group (n=6) received the buffer alone (i.p.) to simulate  
145 the injection stress. Fasting blood glucose levels were measured after 2 days using a glucometer  
146 (Accu-Chek® Performa, Roche LTDA. Jaguaré, SP, Brazil) in blood samples collected at the tail  
147 vein. All STZ-injected animals presented the fasting glycemia levels higher than 250 mg/dL and  
148 were included in the study. The diabetic rats were divided into two groups (n=6, each). Therefore,  
149 the experiment consisted of three groups: the healthy control group (Ctrl, n=6), which received  
150 water as a placebo; the diabetic control group (STZ, n=6), which also received water; and the  
151 diabetic group treated with the green tea infusion (STZ+GTI, n=6), that received the GTI (100

152 mg/kg body weight). All treatments were administered by gavage, daily, for 42 days. The dosage  
153 was equivalent to 7 cups (200mL) of tea, prepared according to the manufacturer instructions,  
154 mimicking a feasible human consumption dosage, considering survey data from the Asian  
155 population (Mineharu et al., 2011).

156 We monitored body weight and water consumption using a precision scale (BEL M503,  
157 e=0.001g, Piracicaba, SP, Brazil), and 12h fasting blood glucose using test strips and a glucometer  
158 (Accu-Chek® Performa, Roche LTDA. Jaguaré, SP, Brazil) in blood samples from the tail vein.

159 After the experimental period, the animals were euthanized by deep anesthesia (sodium  
160 thiopental, 60 mg/kg i.p.) followed by cardiac puncture and exsanguination. The kidneys were  
161 removed and weighed. One kidney (right) of each animal was frozen in liquid nitrogen and stored at  
162 -80 °C for enzymatic analysis, the other one (left) was immersed in Karnovsky fixative solution for  
163 24h for histopathological analyses. The renal somatic index (RSI) was calculated using the ratio  
164 between the kidney weight (KW) and BW, where  $RSI = KW/BW \times 100$  (Sertorio et al., 2019).

165

#### 166 2.4. Renal function markers

167 Blood samples collected by cardiac puncture at the euthanasia were centrifuged at 4600 rpm for  
168 15 min at 4 °C and the serum was separated. Then we performed the analysis for quantification of  
169 urea and creatinine in the serum using biochemical kits (Bioclin Laboratories, Belo Horizonte, MG,  
170 Brazil) at the BS-200 equipment (Bioclin Laboratories, Belo Horizonte, MG, Brazil) following the  
171 manufacturer's instructions.

172

173 *2.5. Antioxidant enzyme and nitric oxide analysis*

174 The antioxidant enzyme analysis was performed with the supernatant obtained from 100 mg of  
175 frozen kidney tissue homogenized in ice-cold phosphate buffer (pH 7.0) and centrifuged at 12000  
176 rpm for 10 minutes at 4 °C. The activity of the superoxide dismutase enzyme (SOD) was assessed  
177 by the pyrogallol method based on the ability of this enzyme to catalyze the reaction of the  
178 superoxide ( $O_2^{\cdot -}$ ) and hydrogen peroxide ( $H_2O_2$ ) (Dieterich et al., 2000). The glutathione S-  
179 transferase (GST) activity was measured according to the method of Habig et al. (1974), and  
180 calculated from the rate of NADPH oxidation. The activity of catalase (CAT) was determined by  
181 measuring the kinetics of hydrogen peroxide ( $H_2O_2$ ) decomposition as described by Aebi (1984).  
182 The nitric oxide ( $NO_2^-$  and  $NO_3^-$ ) levels were quantified by the Griess method (Ricart-Jané et al.,  
183 2002). The values of enzyme activities were normalized by the total protein content, determined  
184 with the Folin–Ciocalteu method according to Lowry et al. (1994).

185  
186 *2.6. Determination of  $Ca^{2+}$ ,  $Na^+/K^+$ ,  $Mg^{2+}$ , and total ATPase activities*

187 The ATPase activity was determined following the procedure described by Al-Numair et al  
188 (2015). Briefly, 100mg of kidney fragments were homogenized in Tris-HCl buffer (0.1M, pH 7.4)  
189 and centrifuged at 12000 rpm for 10 min at 5°C. The supernatant was used for the determination of  
190 the ATPase activity using NaCl, KCl, MgCl, and CaCl solutions at 0.1M. ATP solution (0.1M) was  
191 used as a substrate to generate free phosphate by the ATPases. The reaction was stopped with a cold  
192 solution of 10% TCA. Then, we centrifuged at 6000 rpm for 10 min and the supernatant was used to  
193 determine the inorganic phosphorus content by the Fiske and Subbarow method (Fiske and  
194 Subbarow, 1925). The ATPase activities were expressed as  $\mu$ Mol of inorganic phosphorus/min mg  
195 of protein.

196

## 197 2.7. Chemical elements analysis

198 The proportion of chemical elements in the renal cortex was assessed per area in fragments of  
199 frozen kidney, as described before (Ladeira et al., 2020b). We measured the proportion of sodium  
200 (Na), magnesium (Mg), chlorine (Cl), potassium (K), and calcium (Ca). Fragments were dried at 60  
201 °C for 96h, coated with carbon (Quorum Q150 T, East Grinstead, West Sussex, England, UK), and  
202 analyzed in a scanning electron microscope (JEOL, JSM-6010LA) with a Silicon Drift type X-ray  
203 detector system. The analysis was performed in an area of 50  $\mu\text{m}^2$ , using an accelerating voltage of  
204 20 kV and a working distance of 10 mm. The results were expressed as a mean value of the  
205 proportions between the elements present in the samples.

## 206 2.8. Histopathological and stereological analysis and assessment of DNA damage

207 The fragments fixed in Karnovsky solution were then dehydrated in a crescent ethanol series  
208 and embedded in Histo-resin® (Leica, Nussloch, Germany). A rotary microtome (RM 2255, Leica  
209 Biosystems, Nussloch, Germany) was used to cut the material into histological sections of 3  $\mu\text{m}$   
210 thickness, then, the section was mounted in glass slides and reacted with periodic acid and Schiff  
211 reagent (PAS), and counterstained with hematoxylin for histopathological and stereological  
212 evaluation. The analysis was carried as described before by Sertorio *et al* (2019). Also, slices  
213 stained with Toluidine Blue – Sodium borate 1% were used to analyze qualitatively the glomeruli  
214 morphopathological features. We analyzed 40 glomeruli, randomly photographed, per experimental  
215 animal.

216 DNA damage was evaluated in sections of the kidney cortex stained with acridine orange (AO;  
217 green) and propidium iodide (PI; red) (Bernas et al., 2005; Suzuki et al., 1997). This fluorescent  
218 stain allows to evaluate the DNA damage, as damaged DNA presents red color, marked with PI,  
219 and integral DNA is marked in green by the AO (Dias et al., 2019). Digital images were captured  
220 using a photomicroscope (Olympus AX 70 TRF, Tokyo, Japan) and analyzed with Image-Pro  
221 Plus® 4.5 (Media Cybernetics, Silver Spring, MD) software according to Lima *et al* (2018).

222

223 *2.9. Statistical analysis*

224 All the results were submitted to the Shapiro-Wilk test to check normality. The data expressed  
225 as percentages were transformed by angular transformation before the analysis. Results were  
226 expressed as mean  $\pm$  standard deviation (mean  $\pm$  SD) and analyzed using unpaired *t*-test when the  
227 variances are equal (by *F* test) and unpaired *t*-test with Welch's correction for data with unequal  
228 variances (Ctrl vs STZ; STZ vs STZ+GTI). The non-parametric data were compared with the  
229 Mann-Whitney test. The correlation analysis was carried out following Pearson's correlation  
230 method, as the analyzed data were normally distributed. Statistical significance was established at *P*  
231  $\leq 0.05$ .

232

233 *2.10. In silico pathway exploration*

234 After the in vivo experiment, we explored, through an in silico approach, the interactions of  
235 green tea catechins with proteins, in search of possible signaling pathways involved in the  
236 generation of the observed effects. For this, we built and analyzed a network of interactions based  
237 on information from the STRING and STITCH databases (Szklarczyk et al., 2017, 2016).

238 A chemo-biology interactome network was built to elucidate the interactions between the tea  
239 compounds (catechins) and proteins expressed in the kidneys related to the positive effects founded  
240 in the in vivo experiment with diabetic rats. A prospective evaluation of compound-protein  
241 interactions (CPI) was done with the STITCH v.5.0 database (<http://stitch.embl.de/>) (Szklarczyk et  
242 al., 2016). The CPI settings were done according to (de Godoi et al., 2020). Briefly, the network  
243 downloaded from the database was limited to no more than 50 interactions, medium confidence  
244 score (0.400), network depth equal to 1, and the following methods of predictions were activated:  
245 experiments, databases, co-expression, and predictions. The search was set to retrieve results for

246 seven green tea catechins (Catechin, Catechin gallate, Epicatechin, Epicatechin Gallate,  
247 Epigallocatechin Gallate, Gallocatechin, and Gallocatechin Gallate), using the *Homo sapiens*  
248 species. All the catechins were imputed individually in the search, however, only four (Catechin,  
249 Epicatechin, Epicatechin Gallate, and Epigallocatechin Gallate) retrieve results of interactions,  
250 generating four small CPI subnetworks (data not showed), that were used in the posterior analysis.

251 The four catechin-proteins network analysis was performed using Cytoscape v.3.8.0  
252 (Shannon, 2003). The four subnetworks were merged using the merge tool with the union function  
253 of the software. Then, we “STRINGfy” the resultant network, through the STRING v.1.5.1  
254 (Szklarczyk et al., 2017) to enable the protein interaction functions analysis. After that, we  
255 performed the Molecular Complex Detection analysis to detect clusters (i.e. densely connected  
256 regions) that may suggest functional protein complexes, with the MCODE v.1.6.1 app (Bader and  
257 Hogue, 2003). To that, the app was set up as described before (de Godoi et al., 2020). An MCODE  
258 score was calculated for each cluster. Additionally, the Reactome Pathways (Jassal et al., 2020)  
259 related to diabetic nephropathy pathogenesis were selected.

260 To identify proteins that could be considered as a key regulator of essential biological  
261 processes to the network da network, we performed a centrality analysis, using the CentiScaPe v.2.2  
262 app (Scardoni et al., 2009) for Cytoscape. This app identifies the node (i.e. protein) that has a  
263 central position in the network by measuring the “betweenness” and “degree” of the node. Nodes  
264 with high betweenness and degree levels are named “bottlenecks” and are more probable to connect  
265 different clusters in the network (Yu et al., 2007).

266 The functional information about all the network proteins, as the tissue-specific expression  
267 score and the cellular location score, was accessed by the ClueGO v.2.5.7 and CluePedia v.1.5.7  
268 apps (Bindea et al., 2013, 2009). The Specific Organ Expression Score (SOES) was accessed in this  
269 analysis and a filter to protein expression was used to apply the SOES to the PPI (Protein-Protein  
270 Interactome). Protein functions were accessed in the Human Gene database - GeneCards

271 (<http://www.genecards.org/>) (Rebhan et al., 1998) and compared with the functions related to their  
272 effects in diabetic nephropathy, described in the scientific literature.

273

### 274 3. Results

#### 275 3.1. Experimental results

276 Diabetic animals showed classical signs of polydipsia (Table 1) and polyuria observed  
277 during the experiment (noted in the cage bed). The initial body weight was maintained throughout  
278 the experimental period in the animals of the two diabetic groups, indicating a stagnation in the  
279 body weight gain, and a commitment of the body development by hyperglycemia, when compared  
280 to the healthy control group. Both diabetic groups remain severely hyperglycemic, and green tea  
281 infusion did not reduce blood glucose levels in the treated group.

282 The kidney weight was reduced in the diabetic groups when compared with the Ctrl group  
283 ( $P < 0.0001$ ) and it was reflected in the kidney somatic index ( $P < 0.0001$ ). In addition, this result  
284 may be related to the body development impairment due to hyperglycemia, as showed by  
285 bodyweight reduced values. These data are presented in Table 1.

286 The serological analysis revealed that diabetes increased the serum levels of urea and the  
287 GTI did not act modifying this parameter (Figure 2, A). In the same way, creatinine levels were also  
288 higher in the diabetic groups than the healthy control without effect by GTI treatment (Figure 2, B).

289 The GTI was capable of inducing a higher activity of GST enzyme (Figure 3, C), and nitric  
290 oxide levels were increased in both diabetics groups, without any effect of GTI treatment (Figure 3,  
291 D). The activity of SOD and CAT in the kidney were not impacted by diabetes or GTI treatment in  
292 the kidney.

293 Figure 4 shows the measurements of microelements and ions that participate in the filtration  
294 and reabsorption dynamics in the kidney. Despite diabetes have not affected any of the elements

295 analyzed (Figure 4, A – F), green tea infusion altered Mg and Cl amounts compared to the STZ  
296 group (Figure 4, B and D). Although all altered values (Mg and Cl) remain between the Ctrl normal  
297 reported values, the relationship between all these elements were impaired by diabetes (Figure 4,  
298 G), and GTI was not able to restore the homeostatic environment of ion dynamics. Additionally, we  
299 detected a reduced activity of the  $\text{Na}^+/\text{K}^+$  ATPase pump in the diabetic group (Figure 4, H). The  
300  $\text{Ca}^{2+}$  and  $\text{Mg}^{2+}$  ATPases, as the total ATPase activity were not affected.

301 Histopathological analysis revealed a reduced glomerular volume in the diabetic groups  
302 (Figure 5, C), despite no differences in the glomeruli number per area ( $\text{mm}^2$ ) (Figure 5, B). Sections  
303 of the healthy control group did not show any pathological feature, and the measurements are  
304 compatible with the described ones for the species. However, the diabetic groups presented an  
305 abnormal accumulation of glycogen in the tubules, known as glycogen nephrosis. The volume of  
306 glycogen accumulation in the diabetic group was increased compared with the Ctrl group (Figure 5,  
307 D), however the GTI treatment was able to prevent the glycogen granules accumulation in the  
308 diabetic animals (Figure 5, D).

309 Diabetes led to a reduced proportion of AO-positive cells in the renal cortex (Figure 6, A),  
310 indicating a reduced proportion of cells without DNA damage. A direct consequence of that is the  
311 increased proportion of IP-positive cells, shown in Figure 6, B. On the other hand, GTI was able to  
312 counteract these effects, improving the proportion of AO-positive cells (Figure 6, A), and reducing  
313 the proportion of the IP-positive cells (Figure 6, B).

314 Glomerular morphological analysis reveals diabetic glomerulus surrounded by flattened  
315 epithelial cells, with pathological alterations that were less frequent in the group treated with GTI.  
316 Diffuse mesangial expansion was more frequent, present in almost every glomeruli in the STZ  
317 group. Bowman's capsule lesions were more frequent in the untreated diabetic than in the STZ+GTI  
318 group. Nodular mesangial expansion was not observed in any group. Moderate dilation in the lumen  
319 of the proximal tubule was more frequent in the STZ group. Also in the STZ group, the basal region

320 of the proximal tubular cells presented the accumulation of aggregated stained granules, more  
321 densely than in the healthy group, possible mitochondria aggregation (Itagaki et al., 1995).  
322 Furthermore, karyocytomegaly was frequently observed in the STZ group and less frequency in the  
323 STZ+GTI group, as so as cytoplasmatic microvesicles, possibly lipid droplets, in the proximal  
324 tubule cells (Figure 7).

### 325 3.2. Virtual analysis

326 The STRING network is presented in Figure 8, A, and highlights the two main functional  
327 clusters (Cluster 1 and Cluster 2). The Reactome Pathway analysis for each cluster is summarized in  
328 Table 2. The centrality analysis showed that protein kinase B 1 (AKT1) is the protein classified as  
329 the “bottleneck” in the network and has the capacity to integrate the functional pathways that  
330 participate in the catechins effects in the kidney (Figure 8, B). The implications of AKT1 in green  
331 tea induced signaling in diabetic nephropathy are discussed below. All proteins in the PPI network  
332 are expressed in the normal kidney in different degrees.

333

## 334 4. Discussion

335 Our results showed that green tea infusion treatment was able to prevent glycogen  
336 accumulation in the renal tubules, reduce the DNA damage caused by the hyperglycemic state in  
337 renal cortex cells, and act preventing the aggravation of glomerular morphological alterations,  
338 independently of any hyperglycemia reduction. These outcomes confirm that green tea positive  
339 effects in diabetic nephrosis are broader than glycemic regulation related effects. Although our  
340 study has not shown a strong improvement in organ function, DNA preservation is determinant in  
341 cell survival and proper function, and glomerular morphological integrity is elemental to the  
342 filtration process. Such results, together with the *in silico* considerations, may indicate key points in

343 the signaling pathways to improve diabetic nephropathy treatment, as coadjuvant, and prevention,  
344 with an herbal medicine, widely distributed and highly accepted around the world.

345 In adult animals, the weight of the kidney is increased by the damage caused by  
346 hyperglycemia. Such injuries lead to hypertrophy and compensatory hyperplasia in the tubules, in  
347 order to preserve the glomerular filtration function, thus increasing the kidney's weight (Herman-  
348 Edelstein and Doi, 2016). However, our animals were induced to diabetes at a younger age, so that  
349 they had not passed the full development process of the body and organs, including the kidneys, that  
350 would still go through a period of growth, with subsequent weight gain (Arataki, 1926). The  
351 damage caused by hyperglycemia at this stage of life seems to have been severe enough to delay the  
352 progression of the organ's normal growth, stagnating the weight gain together with the entire body  
353 development of the animal, as described in other experimental conditions with young animals (da  
354 Silva et al., 2016; Haraguchi et al., 2020; Silva et al., 2009). Besides, such damage may have  
355 extended to prevent green tea's positive effects on kidney function markers found in other studies  
356 with adult animals (Hayashi et al., 2020; Renno et al., 2008). Our data suggest that diabetes, when  
357 rises early, impairs the development of the kidney, as well as the glomerulus, reflected in the low  
358 volume of the glomerulus and appearance of pathological features (e.g. mesangial expansion,  
359 karyocytomegaly, and glomerular basal membrane alterations) in the diabetic animals compared to  
360 healthy control. Although we have not observed statistical difference, the size of glomerulus was  
361 observed to have a higher mean and a lower variance (SD) in the group treated with green tea  
362 compared with the diabetic one, approaching the characteristics that describe the control group.  
363 Such data are in line with the protective effects on glomerular morphology exercised by EGCG, the  
364 main catechin found in green tea (Yoon et al., 2014).

365 It is known that catechins in green tea have a hypoglycemic and preventive effect on high  
366 glucose levels (Fu et al., 2017), and it was assumed that the beneficial effects of green tea in  
367 diabetic nephropathy, especially concerning the tubular glycogen nephrosis, were due to this  
368 hypoglycemiant capacity (Renno et al., 2008). However, green tea treatment, or its isolated catechin

369 administration, can generate positive outcomes without the achievement of proper glycemic control  
370 (Hayashi et al., 2020), confirming that tea's effect on diabetes goes beyond improving glucose-  
371 related harms.

372 The glycogen accumulation in renal tubules, as presented in our study, is a hallmark of  
373 experimental diabetic nephropathy induced by STZ or Alloxan in experimental models (Kang et al.,  
374 2005). In normal conditions, glucose is reabsorbed almost completely in the proximal tubule by  
375 sodium-dependent glucose transporter 2 (SGLT2) and, in lower levels, by sodium-dependent  
376 glucose transporter 1 (SGLT1), and appears in the urine when the absorptive capacity is  
377 extrapolated (Bailey, 2011; Vallon and Thomson, 2017). Additionally, proximal tubule cells have a  
378 greater capacity to perform gluconeogenesis from lactate, glutamine, and glycerol, and this is an  
379 upregulated process in diabetes (Eid et al., 2006). The glycogen accumulated in the tubule may  
380 result from the sum of factors including abnormally increased absorption, and increased  
381 gluconeogenesis (Herman-Edelstein and Doi, 2016; Mather and Pollock, 2011).

382 Green tea catechins are shown to act as SGLT1 inhibitors *in vitro* (Kobayashi et al., 2000),  
383 suggesting that tea treatment forces the glucose reabsorption process in the kidney to be done by  
384 SGLT2 alone. At the time, there is no evidence suggesting an inhibitory effect of catechins on  
385 SGLT2. However, EGCG was shown to inhibit glucose production via gluconeogenesis in cells by  
386 activating the AMPK (Collins et al., 2007). Also, EGCG suppresses gluconeogenic gene expression  
387 (e.g. glucose-6-phosphatase and phosphoenolpyruvate carboxykinase) via the phosphoinositide 3-  
388 kinase (PI3K) pathway (Waltner-Law et al., 2002). Such a mechanism in kidney cells could lead to  
389 a reduced glucose overload and the improvement of glycogen accumulation in proximal tubules and  
390 may explain the positive outcomes of GTI treatment in our study.

391 Furthermore, diabetes can increase the expression of SGLT2 and sodium-hydrogen  
392 antiporter 3 (NHE3), in response to the higher demand for adenosine triphosphate (ATP) to  
393 maintain the glucose reabsorption flow (Herman-Edelstein and Doi, 2016). The great capacity of

394 tubular cells to perform gluconeogenesis, a process that consumes a lot of ATP, further increases  
395 the demand for the molecule (Gilbert, 2017). Such increased demand for energy therefore enhances  
396 the oxygen (O<sub>2</sub>) demand creating a hypoxic environment in the tubular cells (Herman-Edelstein and  
397 Doi, 2016). However, the blood supply of O<sub>2</sub> in this case is severely affected by the endothelial  
398 damage caused by glucose, leading to loss and obstruction of capillaries, worsen the oxygen supply  
399 (Herman-Edelstein and Doi, 2016). In this way, a deeper hypoxic environment is generated,  
400 favorable to the activation of apoptosis via the Caspase pathway, and the fibrosis development in  
401 the organ by stimulating the Transforming growth factor-beta (TGF- $\beta$ ) pathway. In turn, the  
402 progression of fibrosis further worsens hypoxia, aggravating cell death in the organ (Gilbert, 2017).  
403 This mechanism is also accompanied by increased expression of stem cell factor (SCF) and  
404 proto-oncogene c-kit (c-kit) (Yin et al., 2018). In contrast, ellagic acid, a derivative polyphenol  
405 found in green tea (Yang and Tomás-Barberán, 2019), is shown to inhibit tyrosinase activity  
406 (Yoshimura et al., 2005) inhibiting the SCT-Kit pathway and alleviating the damages caused by  
407 hypoxia.

408 In this same line, green tea extract can inhibit the fibroblast growth factor receptor (FGFR)  
409 signaling by reducing the expression of fibroblast growth factor (FGF) (Sartippour et al., 2002), and  
410 EGCG impedes the signaling pathway of the platelet-derived growth factor (PDGF), other  
411 profibrotic factors (Park et al., 2006).

412 Hypoxia can aggravate diabetic kidney disease by upregulating the expression of Toll-Like  
413 Receptor 4 (TLR4) ligands in diabetes, as fibronectin (Zhang et al., 2018) and high-mobility group  
414 box 1 (HMGB1) (Feng et al., 2020). The activation of the TLR4 signal mediated by the TIR-  
415 domain-containing adaptor-inducing Interferon- $\beta$  (TRIF) culminate in the activation of the nuclear  
416 factor  $\kappa$  B (NF- $\kappa$ B) that lead to inflammation and fibrosis in the kidney (Feng et al., 2020).  
417 However, EGCG was shown to inhibit the TLR pathway activation *in vitro* (Youn et al., 2006) and  
418 to reduce the NF $\kappa$ B expression (Yamabe et al., 2006) suggesting that tea may act through this  
419 mechanism to promote anti-inflammatory and antifibrotic protection in the kidney.

420 Our results showed that green tea was able to reduce the binding of propidium iodide to  
421 DNA and enhance GST activity, suggesting an improvement in DNA integrity or that there was  
422 some reduction in the damage caused by hyperglycemia or oxidizing agents. A previous study  
423 showed that EGCG can inhibit apoptosis induced by oxidative stress (Itoh et al., 2005) preserving  
424 renal cells in an *in vitro* model. Also, green tea polyphenols can contribute to reduce apoptosis  
425 levels in diabetic nephropathy by blocking the glycogen synthase kinase-3  $\beta$  (GSK3 $\beta$ ) interaction  
426 with the tumor protein 53 (TP53), reducing Caspase 3 activity in podocytes leading to higher cell  
427 survival rates (Borges et al., 2016; Peixoto et al., 2015). A review study by Mohabbulla Mohib et al.  
428 (2016) summarizes other possible mechanisms that green tea protects the nuclear envelope and the  
429 genome, including the stabilization of the DNA strand and also the reduction of NF- $\kappa$ B expression  
430 culminating in the already discussed positive outcomes.

431 The homeostatic maintenance of the ions inside the cell may influence the antioxidant  
432 enzyme activities (Soetan et al., 2010). Our results show that green tea was not able to reverse the  
433 dysregulation in the relationship between the ions in the kidneys, which actively participate in the  
434 functioning of antioxidant enzymes. Also, oxidative stress may be responsible to inhibit Na<sup>+</sup>/K<sup>+</sup>  
435 ATPase activity by oxidation of thiol groups in the pumps (Al-Numair et al., 2015), and despite the  
436 increased GST activity shown in our study, Na<sup>+</sup>/K<sup>+</sup> ATPase function was not recovered.

437 The PI3K/AKT/mammalian target of rapamycin (mTOR) pathway is linked to metabolic  
438 regulation in diabetic nephropathy and also in the development of human kidney cancer. This signal  
439 cascade is upregulated in diabetes and is closely related to glycogen tubular accumulation (Ribback  
440 et al., 2015). EGCG is shown to inhibit both PI3K and mTOR, by competitively binding in the  
441 ATP-binding sites in these proteins (Van Aller et al., 2011). Additionally, mTOR inhibition can  
442 restore the autophagy mechanism, reduced by mTOR overexpression in diabetes, and contribute to  
443 cellular renovation in the kidney. Also, the PI3K/AKT/mTOR pathway is related to *de novo*  
444 lipogenesis in the kidney (Ribback et al., 2015), which can lead to lipid accumulation, as in line

445 with the microvesicles showed in Figure 6 D. Green tea treated animals didn't present this  
446 cytoplasmic microvesicles.

447 Our *in silico* results show that protein kinase B (AKT) is the central protein in the catechin  
448 mediated effects in the kidney. EGCG can activate the diacylglycerol kinase (DGK) pathway,  
449 promoting the inactivation of protein kinase C beta (PKC- $\beta$ ) and improving the condition of  
450 diabetic nephropathy (Hayashi et al., 2020). Such a process is initiated the interaction of EGCG  
451 with the 67-kDa laminin receptor (67LR), which is known as an EGCG receptor (Tachibana et al.,  
452 2004), and is also capable of activating the AKT in the kidney (Kumazoe et al., 2020). Hayashi et al  
453 (2015) showed that EGCG activates DGK- $\alpha$  via 67LR binding. In a recent study (Hayashi et al.,  
454 2020), the authors proposed that this mechanism occurs by activating 67LR receptors in the cell  
455 membrane, which, when activated, promotes the translocation of the DGK to the membrane,  
456 through the formation of 67LR-DGK- $\alpha$  and  $\alpha$ 3- $\beta$ 1 integrin's complex, promoting greater focal  
457 adhesion of podocyte foot process in the glomerular basement membrane, ensuring cell adhesion, in  
458 addition to inhibiting  $\alpha$  and  $\beta$  PKC (Hayashi, 2020), preserving glomerular morphology. This  
459 mechanism may be responsible for the positive effects concerning glomerular preservation by green  
460 tea ingestion. Other catechins present in green tea composition may exert effect by AKT pathway  
461 activation by a different receptor, as they do not bind with the 67LR (Tachibana et al., 2004),  
462 however the primary membrane receptor for them are still unknown.

463

## 464 **5. Conclusion**

465 The components of green tea can interact with proteins participating in cell signaling  
466 pathways that regulate energy metabolism, including glucose and glycogen synthesis, glucose  
467 reabsorption, hypoxia management, and cell death by apoptosis. Such interaction leads to reduced  
468 accumulation of glycogen in the kidney's cells of the proximal tubules in diabetes, as well as to  
469 reduce DNA damage. These results also reflect in a preserved glomerulus morphology, with

470 improvement in pathological features, and suggesting a prevention of kidney function impairment.  
 471 Our results show that such benefits are achieved regardless of the blood glucose status, and are not  
 472 dependent on the reduction of hyperglycemia to be achieved.

473

## 474 Abbreviations

475 67LR - 67kDa laminin receptor; ABTS - 2,2'-Azinobis-[3-ethylbenzthiazoline-6-sulfonic acid]; NOS1 - Nitric Oxide Synthase 1;  
 476 AGE/RAGE - advanced glycated end-products and its receptor; AKT - protein kinase B; AMPK - 5'-AMP-activated protein kinase;  
 477 AO - acridine Orange; APC - APC Regulator Of WNT Signaling Pathway; ATP - adenosine triphosphate; BAX - BCL2 Associated  
 478 X; BCL2 - BCL2 Apoptosis Regulator; BID - BH3 Interacting Domain Death Agonist; BW - body weight; Ca - calcium; CaCl<sub>2</sub> -  
 479 calcium chloride; CASP3 - Caspase 3; CASP8 - Caspase 8; CASP9 - Caspase 9; CAT - catalase; CAV1 - Caveolin 1; CCL2 - C-C  
 480 Motif Chemokine Ligand 2; CDK2 - Cyclin Dependent Kinase 2; CDKN1A - Cyclin Dependent Kinase Inhibitor 1; CIAPIN1 -  
 481 Cytokine Induced Apoptosis Inhibitor 1; c-kit - proto-oncogene c-kit; Cl - chlorine; CPI - compound-protein interactions; CTNNA1  
 482 - Catenin Beta 1; Ctrl - control group; DB02077 - L-N(omega)-nitroarginine-(4R)-amino-L-proline amide (NOS3); DB08019,  
 483 DB08018 and NOS3- Nitric Oxide Synthase 3; DKG - diacylglycerol kinase; DN - Diabetic nephropathy; EGCG - epigallocatechin  
 484 gallate; FGF - fibroblast growth factor; FGFR - fibroblast growth factor receptor; FOS - Fos Proto-Oncogene; FRAP - ferric reducing  
 485 antioxidant power; GSK3β - glycogen synthase kinase-3 β; GST - glutathione S-transferase; GTI - Green tea infusion; H<sub>2</sub>O<sub>2</sub> -  
 486 hydrogen peroxide; H6PD - Hexose-6-Phosphate Dehydrogenase/Glucose 1-Dehydrogenase; HIF1A - Hypoxia Inducible Factor 1  
 487 Subunit Alpha; HMG1 - high-mobility group box 1; HSP90AA1 - Heat Shock Protein 90 Alpha Family Class A Member 1; i.p. -  
 488 intraperitoneal; IL6 - Interleukin 6; IL8 - Interleukin 8; JUN - Jun Proto-Oncogene; K - potassium; KCl - potassium chloride; KW -  
 489 kidney weight; MAP2K1 - Mitogen-Activated Protein Kinase Kinase 1; MAPK1 - Mitogen-Activated Protein Kinase 1; MAPK3 -  
 490 Mitogen-Activated Protein Kinase 3; MAPK8 - Mitogen-Activated Protein Kinase 8; MAPKAPK5 - MAPK Activated Protein  
 491 Kinase 5; Mg - magnesium; MgCl<sub>2</sub> - magnesium chloride; MLH1 - MutL Homolog 1; mTOR - mammalian target of rapamycin;  
 492 MTRR - 5-Methyltetrahydrofolate-Homocysteine Methyltransferase Reductase; Na - sodium; NaCl - sodium chloride; NADPH -  
 493 reduced nicotinamide adenine dinucleotide phosphate; NDOR1 - NADPH-dependent diflavin reductase; NFκB - nuclear factor κ B;  
 494 NO<sub>2</sub><sup>-</sup>/NO<sub>3</sub><sup>-</sup> - nitric oxide; NOS2 - Nitric Oxide Synthase 2; NRIH4 - Nuclear Receptor Subfamily 1 Group H Member 4 ; O<sub>2</sub> -  
 495 oxygen; O<sub>2</sub><sup>-</sup> - superoxide; PARP1 - Poly(ADP-Ribose) Polymerase 1; PDGF - platelet-derived growth factor; PGD -  
 496 Phosphogluconate Dehydrogenase; PGLS - 6-Phosphogluconolactonase; PI - propidium iodide; PI3K - phosphoinositide 3-kinase;  
 497 PIN1 - Peptidylprolyl Cis/Trans Isomerase, NIMA-Interacting 1; PKC-β - protein kinase C beta; POR - Cytochrome P450  
 498 Oxidoreductase; PPI - Protein-Protein Interactome; RPIA - Ribose 5-Phosphate Isomerase A; RSI - renal somatic index; SCF - stem  
 499 cell factor; SD - standard deviation; SGLT1 - sodium-dependent glucose transporter 1; SGLT2 - sodium-dependent glucose  
 500 transporter 2; SOD - superoxide dismutase; SOES - Specific Organ Expression Score; STAT3 - Signal transducer and activator of  
 501 transcription 3; STZ - streptozotocin; TCA - Trichloroacetic acid; TCF7L2 - Transcription Factor 7 Like 2; TE - Trolox equivalent;  
 502 TGF-β - transforming growth factor-beta; TLR4 - toll-like receptor 4; TP53 - tumor protein 53; TRIF - TIR domain-containing  
 503 adaptor-inducing Interferon- β; TYW1 - TRNA-YW Synthesizing Protein 1 Homolog; UBC - Ubiquitin C.

504

## 505 Disclosures

506 The authors have no conflicts of interest to disclose.

507

## 508 Authors' contributions

509 LCML planned and carried the experiment, performed the analysis and interpreted the results,  
 510 wrote the original draft, reviewed and final edited the manuscript. ECS participate in the

511 conceptualization of the experiment, interpretation of results and writing of the manuscript. TAS,  
512 JS, GDAL, performed the analysis, interpreted results, reviewed and approved the final manuscript.  
513 MMN participate in the conceptualization of the experiment, provided resources, reviewed and  
514 approved the final manuscript. RCS and MBF provided resources, participate in the interpretation  
515 of results, reviewed and approved the final manuscript. IRSCM participate in the conceptualization  
516 of the experiment, interpretation of results, supervision and administration of the project, reviewed  
517 and approved the final manuscript.

518

### 519 **Availability of data and material**

520 The datasets used and/or analyzed during the current study are available from the  
521 corresponding author on reasonable request.

522

### 523 **Acknowledgments**

524 The authors are grateful to Bioclin Laboratories for kindly providing the biochemical kits  
525 used in this work; “Laboratório de Microscopia Eletrônica” of the Physics Department of the  
526 Federal University of Viçosa; Eliana Alviarez Gutierrez, for the green tea infusion chemical  
527 analysis; Letícia Monteiro Farias, of the “Laboratório de Biodiversidade” of the Biochemistry and  
528 Molecular Biology of the Federal University of Viçosa, for the chemical analysis in HPLC of the  
529 green tea infusion; Professor Dr. Marcio Roberto Silva, for the statistical insights; Enedina  
530 Sacramento, for the English proofreading service; and Coordenação de Aperfeiçoamento de Pessoal  
531 de Nível Superior (CAPES), for the L. C. M. Ladeira Ph.D. scholarship provided (Procs. Nr.  
532 88882.436984/2019-01).

533

534 **Ethics statement**

535 The use of animals in this study was approved by the Ethics Committee of Animal Use of the  
536 Federal University of Viçosa (CEUA/UFV – protocol number 53/2018).

537

538 **Funding**

539 This paper was supported by a grant from the Brazilian agency Capes (Coordenação de  
540 Aperfeiçoamento de Pessoal de Nível Superior, Procs. Nr. 88882.436984/2019-01) and resources  
541 from the CNPq (Conselho Nacional de Desenvolvimento Científico e Tecnológico, Chamada  
542 UNIVERSAL 2018; Procs. Nr. 431330/2018-2).

543

544 **References**

- 545 Aebi, H., 1984. [13] Catalase in vitro, in: *Methods in Enzymology*, Methods in Enzymology.  
546 Elsevier, pp. 121–126. [https://doi.org/10.1016/S0076-6879\(84\)05016-3](https://doi.org/10.1016/S0076-6879(84)05016-3)
- 547 Al-Numair, K.S., Veeramani, C., Alsaif, M.A., Chandramohan, G., 2015. Influence of kaempferol,  
548 a flavonoid compound, on membrane-bound ATPases in streptozotocin-induced diabetic rats.  
549 *Pharm. Biol.* 53, 1372–1378. <https://doi.org/10.3109/13880209.2014.982301>
- 550 Arataki, M., 1926. On the postnatal growth of the kidney, with special reference to the number and  
551 size of the glomeruli (albino rat). *Am. J. Anat.* 36, 399–436.  
552 <https://doi.org/10.1002/aja.1000360302>
- 553 Bader, G.D., Hogue, C.W.V., 2003. An automated method for finding molecular complexes in large  
554 protein interaction networks. *BMC Bioinformatics* 4, 1–27. [https://doi.org/10.1186/1471-2105-](https://doi.org/10.1186/1471-2105-4-2)  
555 4-2
- 556 Bailey, C.J., 2011. Renal glucose reabsorption inhibitors to treat diabetes. *Trends Pharmacol. Sci.*  
557 32, 63–71. <https://doi.org/10.1016/j.tips.2010.11.011>
- 558 Barkaoui, M., Katiri, A., Boubaker, H., Msanda, F., 2017. Ethnobotanical survey of medicinal  
559 plants used in the traditional treatment of diabetes in Chtouka Ait Baha and Tiznit (Western  
560 Anti-Atlas), Morocco. *J. Ethnopharmacol.* 198, 338–350.  
561 <https://doi.org/10.1016/j.jep.2017.01.023>
- 562 Bernas, T., Asem, E.K., Robinson, J.P., Cook, P.R., Dobrucki, J.W., 2005. Confocal Fluorescence  
563 Imaging of Photosensitised DNA Denaturation in Cell Nuclei. *Photochem. Photobiol.* 33342,  
564 960–969. <https://doi.org/10.1562/2004-11-11-ra-369>
- 565 Bindea, G., Galon, J., Mlecnik, B., 2013. CluePedia Cytoscape plugin: Pathway insights using

- 566 integrated experimental and in silico data. *Bioinformatics* 29, 661–663.  
567 <https://doi.org/10.1093/bioinformatics/btt019>
- 568 Bindea, G., Mlecnik, B., Hackl, H., Charoentong, P., Tosolini, M., Kirilovsky, A., Fridman, W.H.,  
569 Pagès, F., Trajanoski, Z., Galon, J., 2009. ClueGO: A Cytoscape plug-in to decipher  
570 functionally grouped gene ontology and pathway annotation networks. *Bioinformatics* 25,  
571 1091–1093. <https://doi.org/10.1093/bioinformatics/btp101>
- 572 Borges, C.M., Papadimitriou, A., Duarte, D.A., Lopes De Faria, J.M., Lopes De Faria, J.B., 2016.  
573 The use of green tea polyphenols for treating residual albuminuria in diabetic nephropathy: A  
574 double-blind randomised clinical trial. *Sci. Rep.* 6, 1–9. <https://doi.org/10.1038/srep28282>
- 575 Chopade, V. V., Phatak, A.A., Upaganlawar, A.B., Tankar, A.A., 2008. Green tea (*Camellia*  
576 *sinensis*): chemistry , traditional , medicinal uses and its pharmacological activities- a review.  
577 *Pharmacogn. Rev.* 2, 157–162.
- 578 Collins, Q.F., Liu, H.-Y.Y., Pi, J., Liu, Z., Quon, M.J., Cao, W., 2007. Epigallocatechin-3-gallate  
579 (EGCG), A Green Tea Polyphenol, Suppresses Hepatic Gluconeogenesis through 5'-AMP-  
580 activated Protein Kinase. *J. Biol. Chem.* 282, 30143–30149.  
581 <https://doi.org/10.1074/jbc.M702390200>
- 582 da Silva, E., Natali, A.J., da Silva, M.F., de Jesus Gomes, G., da Cunha, D.N.Q., Toledo, M.M.,  
583 Drummond, F.R., Ramos, R.M.S., dos Santos, E.C., Novaes, R.D., de Oliveira, L.L.,  
584 Maldonado, I.R. dos S.C., 2016. Swimming training attenuates the morphological  
585 reorganization of the myocardium and local inflammation in the left ventricle of growing rats  
586 with untreated experimental diabetes. *Pathol. - Res. Pract.* 212, 325–334.  
587 <https://doi.org/10.1016/j.prp.2016.02.005>
- 588 de Godoi, R.S., Almerão, M.P., da Silva, F.R., 2020. In silico evaluation of the antidiabetic activity  
589 of natural compounds from *Hovenia dulcis* Thunberg. *J. Herb. Med.* 100349.  
590 <https://doi.org/10.1016/j.hermed.2020.100349>
- 591 Dias, F.C.R., Martins, A.L.P., de Melo, F.C.S.A., Cupertino, M. do C., Gomes, M. de L.M., de  
592 Oliveira, J.M., Damasceno, E.M., Silva, J., Otoni, W.C., da Matta, S.L.P., 2019.  
593 Hydroalcoholic extract of *Pfaffia glomerata* alters the organization of the seminiferous tubules  
594 by modulating the oxidative state and the microstructural reorganization of the mice testes. *J.*  
595 *Ethnopharmacol.* 233, 179–189. <https://doi.org/10.1016/j.jep.2018.12.047>
- 596 Dieterich, S., Bieligg, U., Beulich, K., Hasenfuss, G., Prestle, J., 2000. Gene Expression of  
597 Antioxidative Enzymes in the Human Heart : Increased Expression of Catalase in the End-  
598 Stage Failing Heart. *Circulation* 101, 33–39. <https://doi.org/10.1161/01.CIR.101.1.33>
- 599 Eid, A., Bodin, S., Ferrier, B., Delage, H., Boghossian, M., Martin, M., Baverel, G., Conjard, A.,  
600 2006. Intrinsic gluconeogenesis is enhanced in renal proximal tubules of Zucker diabetic fatty  
601 rats. *J. Am. Soc. Nephrol.* 17, 398–405. <https://doi.org/10.1681/ASN.2005070742>
- 602 Fallah Huseini, H., Fakhrzadeh, H., Larijani, B., Shikh Samani, A.H., 2006. Review of anti-diabetic  
603 medicinal plant used in traditional medicine. *J. Med. Plants* 5, 1–8.
- 604 Feng, Q., Liu, D., Lu, Y., Liu, Z., 2020. The Interplay of Renin-Angiotensin System and Toll-Like  
605 Receptor 4 in the Inflammation of Diabetic Nephropathy. *J. Immunol. Res.* 2020, 1–11.  
606 <https://doi.org/10.1155/2020/6193407>
- 607 Fiske, C.C.H., Subbarow, Y.Y., 1925. The colorimetric determination of phosphorus. *J. Biol.*  
608 *Chem.* 66, 375–400.
- 609 Fu, Q.-Y., Li, Q.-S., Lin, X.-M., Qiao, R.-Y., Yang, R., Li, X.-M., Dong, Z.-B., Xiang, L.-P.,

- 610 Zheng, X.-Q., Lu, J.-L., Yuan, C.-B., Ye, J.-H., Liang, Y.-R., 2017. Antidiabetic Effects of  
611 Tea. *Molecules* 22, 849. <https://doi.org/10.3390/molecules22050849>
- 612 Gilbert, R.E., 2017. Proximal tubulopathy: Prime mover and key therapeutic target in diabetic  
613 kidney disease. *Diabetes* 66, 791–800. <https://doi.org/10.2337/db16-0796>
- 614 Habig, W.H., Pabst, M.J., Jakoby, W.B., 1974. Glutathione S-Transferases: The first enzymatic step  
615 in mercapturic acid formation. *J. Biol. Chem.* 25, 7130–7139.
- 616 Haraguchi, R., Kohara, Y., Matsubayashi, K., Kitazawa, R., Kitazawa, S., 2020. New Insights into  
617 the Pathogenesis of Diabetic Nephropathy: Proximal Renal Tubules Are Primary Target of  
618 Oxidative Stress in Diabetic Kidney. *Acta Histochem. Cytochem.* 53, 21–31.  
619 <https://doi.org/10.1267/ahc.20008>
- 620 Hayashi, D., Ueda, S., Yamanoue, M., Saito, N., Ashida, H., Shirai, Y., 2015. Epigallocatechin-3-  
621 gallate activates diacylglycerol kinase alpha via a 67 kDa laminin receptor: A possibility of  
622 galloylated catechins as functional food to prevent and/or improve diabetic renal dysfunctions.  
623 *J. Funct. Foods* 15, 561–569. <https://doi.org/10.1016/j.jff.2015.04.005>
- 624 Hayashi, D., Wang, L., Ueda, S., Yamanoue, M., Ashida, H., Shirai, Y., 2020. The mechanisms of  
625 ameliorating effect of a green tea polyphenol on diabetic nephropathy based on diacylglycerol  
626 kinase  $\alpha$ . *Sci. Rep.* 10, 1–12. <https://doi.org/10.1038/s41598-020-68716-6>
- 627 Herman-Edelstein, M., Doi, S.Q., 2016. Pathophysiology of diabetic nephropathy, Proteinuria:  
628 Basic Mechanisms, Pathophysiology and Clinical Relevance. Elsevier Inc.  
629 [https://doi.org/10.1007/978-3-319-43359-2\\_4](https://doi.org/10.1007/978-3-319-43359-2_4)
- 630 Itagaki, S. ichi, Nishida, E., Lee, M.J., Doi, K., 1995. Histopathology of subacute renal lesions in  
631 mice induced by streptozotocin. *Exp. Toxicol. Pathol.* 47, 485–491.  
632 [https://doi.org/10.1016/S0940-2993\(11\)80332-5](https://doi.org/10.1016/S0940-2993(11)80332-5)
- 633 Itoh, Y., Yasui, T., Okada, A., Tozawa, K., Hayashi, Y., Kohri, K., 2005. Examination of the anti-  
634 oxidative effect in renal tubular cells and apoptosis by oxidative stress. *Urol. Res.* 33, 261–  
635 266. <https://doi.org/10.1007/s00240-005-0465-7>
- 636 Jassal, B., Matthews, L., Viteri, G., Gong, C., Lorente, P., Fabregat, A., Sidiropoulos, K., Cook, J.,  
637 Gillespie, M., Haw, R., Loney, F., May, B., Milacic, M., Rothfels, K., Sevilla, C., Shamovsky,  
638 V., Shorser, S., Varusai, T., Weiser, J., Wu, G., Stein, L., Hermjakob, H., D'Eustachio, P.,  
639 2020. The reactome pathway knowledgebase. *Nucleic Acids Res.* 48, D498–D503.  
640 <https://doi.org/10.1093/nar/gkz1031>
- 641 Kang, J., Dai, X.-S., Yu, T.-B., Wen, B., Yang, Z.-W., 2005. Glycogen accumulation in renal  
642 tubules, a key morphological change in the diabetic rat kidney. *Acta Diabetol.* 42, 110–116.  
643 <https://doi.org/10.1007/s00592-005-0188-9>
- 644 Kim-Park, W.K., Allam, E.S., Palasuk, J., Kowolik, M., Park, K.K., Windsor, L.J., 2016. Green tea  
645 catechin inhibits the activity and neutrophil release of Matrix Metalloproteinase-9. *J. Tradit.*  
646 *Complement. Med.* 6, 343–346. <https://doi.org/10.1016/j.jtcme.2015.02.002>
- 647 Kobayashi, Y., Suzuki, M., Satsu, H., Arai, S., Hara, Y., Suzuki, K., Miyamoto, Y., Shimizu, M.,  
648 2000. Green Tea Polyphenols Inhibit the Sodium-Dependent Glucose Transporter of Intestinal  
649 Epithelial Cells by a Competitive Mechanism. *J. Agric. Food Chem.* 48, 5618–5623.  
650 <https://doi.org/10.1021/jf0006832>
- 651 Kumazoe, M., Fujimura, Y., Tachibana, H., 2020. 67-kDa Laminin Receptor Mediates the  
652 Beneficial Effects of Green Tea Polyphenol EGCG. *Curr. Pharmacol. Reports.*  
653 <https://doi.org/10.1007/s40495-020-00228-3>

- 654 Ladeira, L.C.M., dos Santos, E.C., Mendes, B.F., Gutierrez, E.A., Santos, C.F.F., de Souza, F.B.,  
655 Machado-Neves, M., Maldonado, I.R. dos S.C., 2020a. Green tea infusion aggravates  
656 nutritional status of the juvenile untreated STZ-induced type 1 diabetic rat. *bioRxiv* 35.  
657 <https://doi.org/10.1101/2020.01.13.904896>
- 658 Ladeira, L.C.M., dos Santos, E.C., Valente, G.E., da Silva, J., Santos, T.A., dos Santos Costa  
659 Maldonado, I.R., 2020b. Could biological tissue preservation methods change chemical  
660 elements proportion measured by energy dispersive X-ray spectroscopy? *Biol. Trace Elem.*  
661 *Res.* 196, 168–172. <https://doi.org/10.1007/s12011-019-01909-x>
- 662 Lima, G.D. de A., Sertorio, M.N., Souza, A.C.F., Menezes, T.P., Mouro, V.G.S., Gonçalves, N.M.,  
663 Oliveira, J.M. de, Henry, M., Machado-Neves, M., 2018. Fertility in male rats: Disentangling  
664 adverse effects of arsenic compounds. *Reprod. Toxicol.* 78, 130–140.  
665 <https://doi.org/10.1016/j.reprotox.2018.04.015>
- 666 Lowry, O.H., Rosebrough, N.J., Farr, A.L., Randal, R.J., 1994. Protein Measurement with the Folin  
667 Phenol Reagent. *Anal. Biochem.* 217, 220–230. [https://doi.org/10.1016/0304-3894\(92\)87011-4](https://doi.org/10.1016/0304-3894(92)87011-4)
- 668 Mather, A., Pollock, C., 2011. Glucose handling by the kidney. *Kidney Int.* 79, S1–S6.  
669 <https://doi.org/10.1038/ki.2010.509>
- 670 Meng, J.-M., Cao, S.-Y., Wei, X.-L., Gan, R.-Y., Wang, Y.-F., Cai, S.-X., Xu, X.-Y., Zhang, P.-Z.,  
671 Li, H.-B., 2019. Effects and Mechanisms of Tea for the Prevention and Management of  
672 Diabetes Mellitus and Diabetic Complications: An Updated Review. *Antioxidants* 8, 170.  
673 <https://doi.org/10.3390/antiox8060170>
- 674 Mineharu, Y., Koizumi, A., Wada, Y., Iso, H., Watanabe, Y., Date, C., Yamamoto, A., Kikuchi, S.,  
675 Inaba, Y., Toyoshima, H., Kondo, T., Tamakoshi, A., 2011. Coffee, green tea, black tea and  
676 oolong tea consumption and risk of mortality from cardiovascular disease in Japanese men and  
677 women. *J. Epidemiol. Community Health* 65, 230–240.  
678 <https://doi.org/10.1136/jech.2009.097311>
- 679 Mohabbulla Mohib, M., Fazla Rabby, S.M., Paran, T.Z., Mehedee Hasan, M., Ahmed, I., Hasan,  
680 N., Abu Taher Sagor, M., Mohiuddin, S., 2016. Protective role of green tea on diabetic  
681 nephropathy - A review. *Cogent Biol.* 2. <https://doi.org/10.1080/23312025.2016.1248166>
- 682 Park, J.S., Kim, M.H., Chang, H.J., Kim, K.M., Kim, S.M., Shin, B.A., Ahn, B.W., Jung, Y.D.,  
683 2006. Epigallocatechin-3-gallate inhibits the PDGF-induced VEGF expression in human  
684 vascular smooth muscle cells via blocking PDGF receptor and Erk-1/2. *Int. J. Oncol.* 29,  
685 1247–1252. <https://doi.org/10.3892/ijo.29.5.1247>
- 686 Peixoto, E.B., Papadimitriou, A., Teixeira, D.A.T., Montemurro, C., Duarte, D.A., Silva, K.C.,  
687 Joazeiro, P.P., Lopes de Faria, J.M., Lopes de Faria, J.B., 2015. Reduced LRP6 expression and  
688 increase in the interaction of GSK3 $\beta$  with p53 contribute to podocyte apoptosis in diabetes  
689 mellitus and are prevented by green tea. *J. Nutr. Biochem.* 26, 416–430.  
690 <https://doi.org/10.1016/j.jnutbio.2014.11.012>
- 691 Perva-Uzunalić, A., Škerget, M., Knez, Ž., Weinreich, B., Otto, F., Grüner, S., 2006. Extraction of  
692 active ingredients from green tea (*Camellia sinensis*): Extraction efficiency of major catechins  
693 and caffeine. *Food Chem.* 96, 597–605. <https://doi.org/10.1016/j.foodchem.2005.03.015>
- 694 Rachid, A., Rabah, D., Farid, L., Zohra, S.F., Houcine, B., 2012. Ethnopharmacological survey of  
695 medicinal plants used in the traditional treatment of diabetes mellitus in the North Western and  
696 South Western Algeria. *J. Med. Plants Res.* 6, 2041–2050.  
697 <https://doi.org/10.5897/JMPR11.1796>
- 698 Rebhan, M., Chalifa-Caspi, V., Prilusky, J., Lancet, D., 1998. GeneCards: A novel functional

- 699 genomics compendium with automated data mining and query reformulation support.  
700 *Bioinformatics* 14, 656–664. <https://doi.org/10.1093/bioinformatics/14.8.656>
- 701 Renno, W.M., Abdeen, S., Alkhalaf, M., Asfar, S., 2008. Effect of green tea on kidney tubules of  
702 diabetic rats. *Br. J. Nutr.* 100, 652–659. <https://doi.org/10.1017/S0007114508911533>
- 703 Ribback, S., Cigliano, A., Kroeger, N., Pilo, M.G., Terracciano, L., Burchardt, M., Bannasch, P.,  
704 Calvisi, D.F., Dombrowski, F., 2015. PI3K/AKT/mTOR pathway plays a major pathogenetic  
705 role in glycogen accumulation and tumor development in renal distal tubules of rats and men.  
706 *Oncotarget* 6, 13036–13048. <https://doi.org/10.18632/oncotarget.3675>
- 707 Ricart-Jané, D., Llobera, M., López-Tejero, M.D., 2002. Anticoagulants and other preanalytical  
708 factors interfere in plasma nitrate/nitrite quantification by the Griess method. *Nitric Oxide -*  
709 *Biol. Chem.* 6, 178–185. <https://doi.org/10.1006/niox.2001.0392>
- 710 Sartippour, M.R., Heber, D., Zhang, L., Beatty, P., Elashoff, D., Elashoff, R., Go, V.L., Brooks,  
711 M.N., 2002. Inhibition of fibroblast growth factors by green tea. *Int. J. Oncol.* 21, 487–491.  
712 <https://doi.org/10.3892/ijo.21.3.487>
- 713 Scardoni, G., Petterlini, M., Laudanna, C., 2009. Analyzing biological network parameters with  
714 CentiScaPe. *Bioinformatics* 25, 2857–2859. <https://doi.org/10.1093/bioinformatics/btp517>
- 715 Sertorio, M.N., Souza, A.C.F., Bastos, D.S.S., Santos, F.C., Ervilha, L.O.G., Fernandes, K.M., de  
716 Oliveira, L.L., Machado-Neves, M., 2019. Arsenic exposure intensifies glycogen nephrosis in  
717 diabetic rats. *Environ. Sci. Pollut. Res.* 26, 12459–12469. <https://doi.org/10.1007/s11356-019-04597-1>
- 719 Shannon, P., 2003. Cytoscape: A Software Environment for Integrated Models of Biomolecular  
720 Interaction Networks. *Genome Res.* 13, 2498–2504. <https://doi.org/10.1101/gr.1239303>
- 721 Silva, M.J., Brodt, M.D., Lynch, M.A., McKenzie, J.A., Tanouye, K.M., Nyman, J.S., Wang, X.,  
722 2009. Type 1 Diabetes in Young Rats Leads to Progressive Trabecular Bone Loss, Cessation  
723 of Cortical Bone Growth, and Diminished Whole Bone Strength and Fatigue Life. *J. Bone*  
724 *Miner. Res.* 24, 1618–1627. <https://doi.org/10.1359/jbmr.090316>
- 725 Soetan, K.O., Olaiya, C.O., Oyewole, O.E., 2010. The importance of mineral elements for humans ,  
726 domestic animals and plants : A review. *African J. Food Sci.* 4, 200–222.
- 727 Su, J., Ye, D., Gao, C., Huang, Q., Gui, D., 2020. Mechanism of progression of diabetic kidney  
728 disease mediated by podocyte mitochondrial injury. *Mol. Biol. Rep.*  
729 <https://doi.org/10.1007/s11033-020-05749-0>
- 730 Suzuki, T., Fujikura, K., Higashiyama, T., Takata, K., 1997. DNA staining for fluorescence and  
731 laser confocal microscopy. *J. Histochem. Cytochem.* 45, 49–53.  
732 <https://doi.org/10.1177/002215549704500107>
- 733 Szklarczyk, D., Morris, J.H., Cook, H., Kuhn, M., Wyder, S., Simonovic, M., Santos, A.,  
734 Doncheva, N.T., Roth, A., Bork, P., Jensen, L.J., Von Mering, C., 2017. The STRING  
735 database in 2017: Quality-controlled protein-protein association networks, made broadly  
736 accessible. *Nucleic Acids Res.* 45, D362–D368. <https://doi.org/10.1093/nar/gkw937>
- 737 Szklarczyk, D., Santos, A., Von Mering, C., Jensen, L.J., Bork, P., Kuhn, M., 2016. STITCH 5:  
738 Augmenting protein-chemical interaction networks with tissue and affinity data. *Nucleic Acids*  
739 *Res.* 44, D380–D384. <https://doi.org/10.1093/nar/gkv1277>
- 740 Tachibana, H., Koga, K., Fujimura, Y., Yamada, K., 2004. A receptor for green tea polyphenol  
741 EGCG. *Nat. Struct. Mol. Biol.* 11, 380–381. <https://doi.org/10.1038/nsmb743>

- 742 Vallon, V., Thomson, S.C., 2017. Targeting renal glucose reabsorption to treat hyperglycaemia: the  
743 pleiotropic effects of SGLT2 inhibition. *Diabetologia* 60, 215–225.  
744 <https://doi.org/10.1007/s00125-016-4157-3>
- 745 Van Aller, G.S., Carson, J.D., Tang, W., Peng, H., Zhao, L., Copeland, R.A., Tummino, P.J., Luo,  
746 L., 2011. Epigallocatechin gallate (EGCG), a major component of green tea, is a dual  
747 phosphoinositide-3-kinase/mTOR inhibitor. *Biochem. Biophys. Res. Commun.* 406, 194–199.  
748 <https://doi.org/10.1016/j.bbrc.2011.02.010>
- 749 Vaz, S.R., de Amorim, L.M.N., de Nascimento, P.V.F., Veloso, V.S.P., Nogueira, M.S., Castro,  
750 I.A., Mota, J.F., Botelho, P.B., 2018. Effects of green tea extract on oxidative stress and renal  
751 function in diabetic individuals: A randomized, double-blinded, controlled trial. *J. Funct.*  
752 *Foods* 46, 195–201. <https://doi.org/10.1016/j.jff.2018.04.059>
- 753 Waltner-Law, M.E., Wang, X.L., Law, B.K., Hall, R.K., Nawano, M., Granner, D.K., 2002.  
754 Epigallocatechin Gallate, a Constituent of Green Tea, Represses Hepatic Glucose Production.  
755 *J. Biol. Chem.* 277, 34933–34940. <https://doi.org/10.1074/jbc.M204672200>
- 756 Yamabe, N., Yokozawa, T., Oya, T., Kim, M., 2006. Therapeutic Potential of (-)-Epigallocatechin  
757 3- O -Gallate on Renal Damage in Diabetic Nephropathy Model Rats. *J. Pharmacol. Exp. Ther.*  
758 319, 228–236. <https://doi.org/10.1124/jpet.106.107029>
- 759 Yang, X., Tomás-Barberán, F.A., 2019. Tea Is a Significant Dietary Source of Ellagitannins and  
760 Ellagic Acid. *J. Agric. Food Chem.* 67, 5394–5404. <https://doi.org/10.1021/acs.jafc.8b05010>
- 761 Yin, D.D., Luo, J.H., Zhao, Z.Y., Liao, Y.J., Li, Y., 2018. Tranilast prevents renal interstitial  
762 fibrosis by blocking mast cell infiltration in a rat model of diabetic kidney disease. *Mol. Med.*  
763 *Rep.* 17, 7356–7364. <https://doi.org/10.3892/mmr.2018.8776>
- 764 Yokozawa, T., Noh, J.S., Park, C.H., 2012. Green tea polyphenols for the protection against renal  
765 damage caused by oxidative stress. *Evidence-based Complement. Altern. Med.* 2012.  
766 <https://doi.org/10.1155/2012/845917>
- 767 Yoon, S.P., Maeng, Y.H., Hong, R., Lee, B.R., Kim, C.G., Kim, H.L., Chung, J.H., Shin, B.C.,  
768 2014. Protective effects of epigallocatechin gallate (EGCG) on streptozotocin-induced diabetic  
769 nephropathy in mice. *Acta Histochem.* 116, 1210–1215.  
770 <https://doi.org/10.1016/j.acthis.2014.07.003>
- 771 Yoshimura, M., Watanabe, Y., Kasai, K., Yamakoshi, J., Koga, T., 2005. Inhibitory effect of an  
772 ellagic acid-rich pomegranate extract on tyrosinase activity and ultraviolet-induced  
773 pigmentation. *Biosci. Biotechnol. Biochem.* 69, 2368–2373.  
774 <https://doi.org/10.1271/bbb.69.2368>
- 775 Youn, H.S., Lee, J.Y., Saitoh, S.I., Miyake, K., Kang, K.W., Choi, Y.J., Hwang, D.H., 2006.  
776 Suppression of MyD88- and TRIF-dependent signaling pathways of toll-like receptor by (-)-  
777 epigallocatechin-3-gallate, a polyphenol component of green tea. *Biochem. Pharmacol.* 72,  
778 850–859. <https://doi.org/10.1016/j.bcp.2006.06.021>
- 779 Yu, H., Kim, P.M., Sprecher, E., Trifonov, V., Gerstein, M., 2007. The importance of bottlenecks in  
780 protein networks: Correlation with gene essentiality and expression dynamics. *PLoS Comput.*  
781 *Biol.* 3, 713–720. <https://doi.org/10.1371/journal.pcbi.0030059>
- 782 Zhang, X., Guo, K., Xia, F., Zhao, X., Huang, Z., Niu, J., 2018. FGF23 C-tail improves diabetic  
783 nephropathy by attenuating renal fibrosis and inflammation. *BMC Biotechnol.* 18, 1–9.  
784 <https://doi.org/10.1186/s12896-018-0449-7>

786

787

788

789

790 **Figure captions**

791 **Figure 1.** Chromatogram of the green tea infusion (*Camellia sinensis*). In detail: peak of the major  
792 compound (Epigallocatechin gallate).

793

794 **Figure 2.** Renal function markers of male Wistar diabetic rats treated or not with green tea infusion  
795 and a healthy control group. **A** – Urea (mg/dL). **B** – Creatinine (mg/dL). Mean  $\pm$  SD. The statistical  
796 differences are indicated with lines with the *P*-value above or below them. Data were compared by  
797 Student *t*-test (Ctrl vs STZ; STZ vs STZ+GTI) considering statistical differences when  $P \leq 0.05$ . (n  
798 = 6 animals/group).

799

800 **Figure 3.** Antioxidant enzymes and nitric oxide levels of male Wistar diabetic rats treated or not  
801 with green tea infusion and a healthy control group. **A** – Superoxide dismutase. **B** – Catalase. **C** –  
802 Glutathione S-Transferase. **D** – Nitric oxide. Mean  $\pm$  SD. The statistical differences are indicated  
803 with lines with the *P*-value above or below them. Data were compared by Student *t*-test (Ctrl vs  
804 STZ; STZ vs STZ+GTI) considering statistical differences when  $P \leq 0.05$ . (n = 6 animals/group).

805

806 **Figure 4.** Microelement proportions and its correlations, and ATPase activity in the kidney of male  
807 Wistar diabetic rats treated or not with green tea infusion and a healthy control group. **A** – Sodium  
808 (%). **B** – Magnesium (%). **C** – Phosphorus (%). **D** – Chlorine (%). **E** – Potassium (%). **F** – Calcium  
809 (%). **G** – Elemental correlations. **H** -  $\text{Na}^+/\text{K}^+$ ,  $\text{Ca}^{2+}$ ,  $\text{Mg}^{2+}$  and total ATPase activity. Mean  $\pm$  SD.

810 The statistical differences are indicated with lines with the  $P$ -value above or below them. Data were  
811 compared by Student  $t$ -test (Ctrl vs STZ; STZ vs STZ+GTI) considering statistical differences when  
812  $P \leq 0.05$ . The correlations were calculated by Pearson's method and the  $r^2$  is shown in the upper  
813 number of each graph cell, the bottom number in each graph cell corresponds to the  $P$ -value of each  
814 correlation. (n = 6 animals/group).

815

816 **Figure 5.** Representative PAS stained photomicrographs, histopathological and stereological  
817 parameters of the kidney's cortex of male Wistar diabetic rats treated or not with green tea infusion  
818 and a healthy control group. **A** – Kidney's cortex photomicrography. The glomeruli are delimited  
819 by the dotted line. The glycogen nephrosis areas are indicated by the arrowheads. The scale bar is  
820 indicated in the figure. **B** – Glomeruli / mm<sup>2</sup>. **C** – Total glomerular volume (mm<sup>3</sup>). **D** – Glycogen  
821 nephrosis volume (mm<sup>3</sup>). The box represents the interquartile interval with the median indicated  
822 (horizontal line), and the whiskers represent the superior and inferior quartiles. The statistical  
823 differences are indicated with lines with the  $P$ -value above or below them. Data were compared by  
824 Student  $t$ -test (Ctrl vs STZ; STZ vs STZ+GTI) considering statistical differences when  $P \leq 0.05$ . (n  
825 = 6 animals/group).

826

827 **Figure 6.** Representative acridine orange (AO) and propidium iodide (IP) stained photomicrographs  
828 of the kidney's cortex of male Wistar diabetic rats treated or not with green tea infusion and a  
829 healthy control group. **A** – Kidney's cortex photomicrography. Green nuclei – AO-positive; Yellow  
830 to reddish nuclei – IP-positive; Arrows indicate PI-positive nuclei. Scales bars are indicated in the  
831 figure. **B** – AO-positive cells (%). **C** – IP-positive cells (%). Mean  $\pm$  SD. The statistical differences  
832 are indicated with lines with the  $P$ -value above them. Data were compared by Student  $t$ -test (Ctrl vs  
833 STZ; STZ vs STZ+GTI) considering statistical differences when  $P \leq 0.05$ . (n = 6 animals/group).

834

835 **Figure 7.** Representative photomicrographs of the glomerulus, stained with Toluidine Blue –  
836 Sodium borate 1%, of male Wistar diabetic rats treated or not with green tea infusion and a healthy  
837 control group. **A** – A normal glomeruli of an animal from the healthy control group. **B** – Diabetic  
838 glomeruli. Arrowhead indicates a thickening in the glomeruli basal membrane. **C** – Diabetic  
839 glomeruli. Arrow indicates a region of diffuse mesangial expansion. **D** – Diabetic glomeruli. Thick  
840 arrow indicates a remarkable vacuolization in the macula densa region. Thin arrows indicate  
841 cytoplasmic microvesicles in the proximal tubule cells. **E** – Diabetic glomeruli. Squares indicate  
842 karyocytomegaly in the proximal tubule. Dotted circles indicate basal regions in the tubular cells  
843 with accumulation of stained granules, possible mitochondria aggregation. The glomeruli present a  
844 dilated Bowman's space.

845

846 **Figure 8.** *In silico* exploration of catechins effects in the kidney. **A** – Compound-Protein  
847 Interactome network, highlighting tea catechins (green nodes), bottleneck protein (red node), cluster  
848 1 (grey nodes), and cluster 2 (light blue nodes). **B** – Centrality analysis for the CPI network, the  
849 blue lines represent the threshold of the parameter.

850

851

852

853

854

855

856

857

858

859

860

861

862

863

864

865

866

867

868

869 **Table 1.**

870 Blood Glucose, biometric parameters and water consumption of male Wistar diabetic rats treated or

871 not with green tea infusion and a healthy control group.

	Ctrl	STZ	STZ+GTI
Blood Glucose (mg/dL)	85.38 ± 7.53	475.00 ± 33.14*	542.80 ± 42.20 <sup>#</sup>
Initial body weight (g)	84.26 ± 14.97	81.27 ± 9.46	81.75 ± 7.57
Final body weight (g)	288.10 ± 44.16	93.08 ± 23.42*	99.75 ± 13.04
Body weight gain (g)	203.80 ± 30.81	11.82 ± 21.87*	18.00 ± 16.18
Kidney weight (g)	0.98 ± 0.07	0.78 ± 0.18 <sup>#</sup>	0.86 ± 0.08
Renal somatic index (%)	0.34 ± 0.05	0.84 ± 0.13*	0.87 ± 0.10
Initial water consumption (mL/day)	44.45 ± 10.02	44.48 ± 9.87	41.78 ± 11.16
Final water consumption (mL/day)	39.25 ± 6.13	118.8 ± 17.45*	139.8 ± 10.26 <sup>#</sup>

872 Mean ± SD. Data were compared by Student *t*-test (Ctrl vs STZ; STZ vs STZ+GTI) considering873 statistical differences when  $P \leq 0.05$ . Asterisk (\*) indicates difference with  $P < 0.0001$ , and the874 hash (#) indicates different means with  $P < 0.05$ . (n = 6 animals/group).

875

876

877

878

879

880

881

882

883 **Table 2.**

884 Reactome pathways identified for each cluster with specific interest to the diabetic nephropathy  
 885 pathological state, identified by the comparison of the CPI network with the Reactome Pathway  
 886 database with the corresponding adjusted *P*-values.

Cluster	Proteins	Reactome Pathway	Adjusted <i>P</i> -value
Cluster 1	NR1H4, CCL2, IL8, IL6,	Apoptosis	$1.76 \times 10^{-7}$
	MAPKAPK5, STAT3, PIN1,	Signaling by SCF-KIT	$1.06 \times 10^{-6}$
	PARP1, CASP8, MTOR, MAPK3,	Signaling by FGFR in disease	$4.35 \times 10^{-6}$
	MAPK8, MLH1, CASP3, CASP9,	Signaling by PDGF	$6.00 \times 10^{-6}$
	GSK3B, HIF1A, BID, MAPK1,	TRIF-mediated TLR3/TLR4 signaling	$6.00 \times 10^{-6}$
	MAP2K1, BAX, BCL2, FOS, JUN, APC, AKT1, CDKN1A, CDK2, TP53, CTNNB1, TCF7L2	AKT phosphorylates targets in the cytosol	$1.15 \times 10^{-5}$
Cluster 2	DB02077, RPIA, POR, H6PD,	eNOS activation	$1.05 \times 10^{-6}$
	PGLS, PGD, AKT1, TYW1,	Pentose phosphate pathway	$1.30 \times 10^{-5}$
	MTRR, NOS2, DB08019,	AKT phosphorylates targets in the cytosol	$3.70 \times 10^{-5}$
	DB08018, AC1NDS4X, NOS1,	Metabolism of carbohydrates	$1.53 \times 10^{-4}$
	CAV1, NDOR1, CIAPIN1,	Cellular response to hypoxia	$1.50 \times 10^{-3}$
	HSP90AA1, UBC, NOS3	PI3K/AKT/mTOR activation	$6.29 \times 10^{-3}$

887

888

889

890

891

892

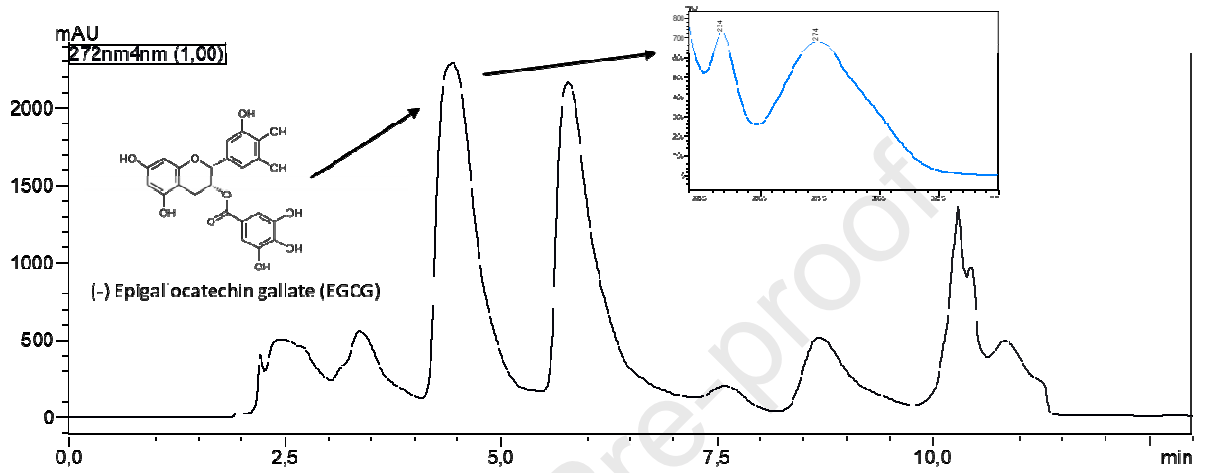
893

894

895

896

897



898

899

Figure 1

900

901

902

903

904

905

906

907

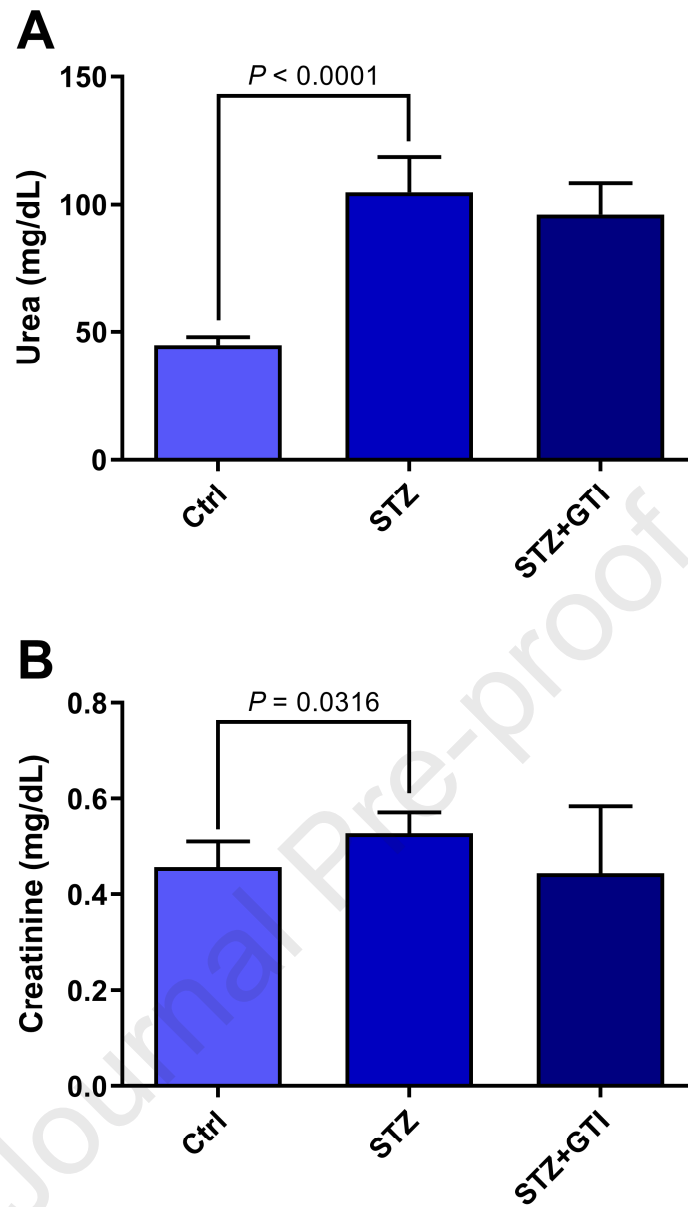


Figure 2

908

909

910

911

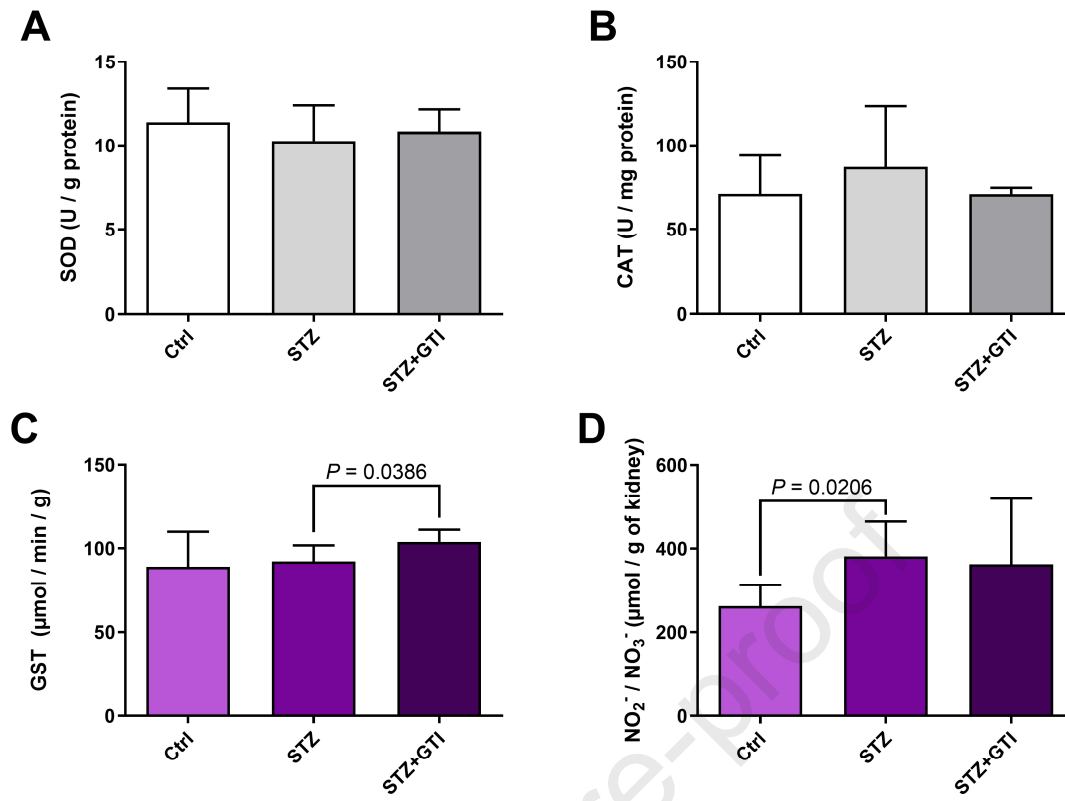


Figure 3

912

913

914

915

916

917

918

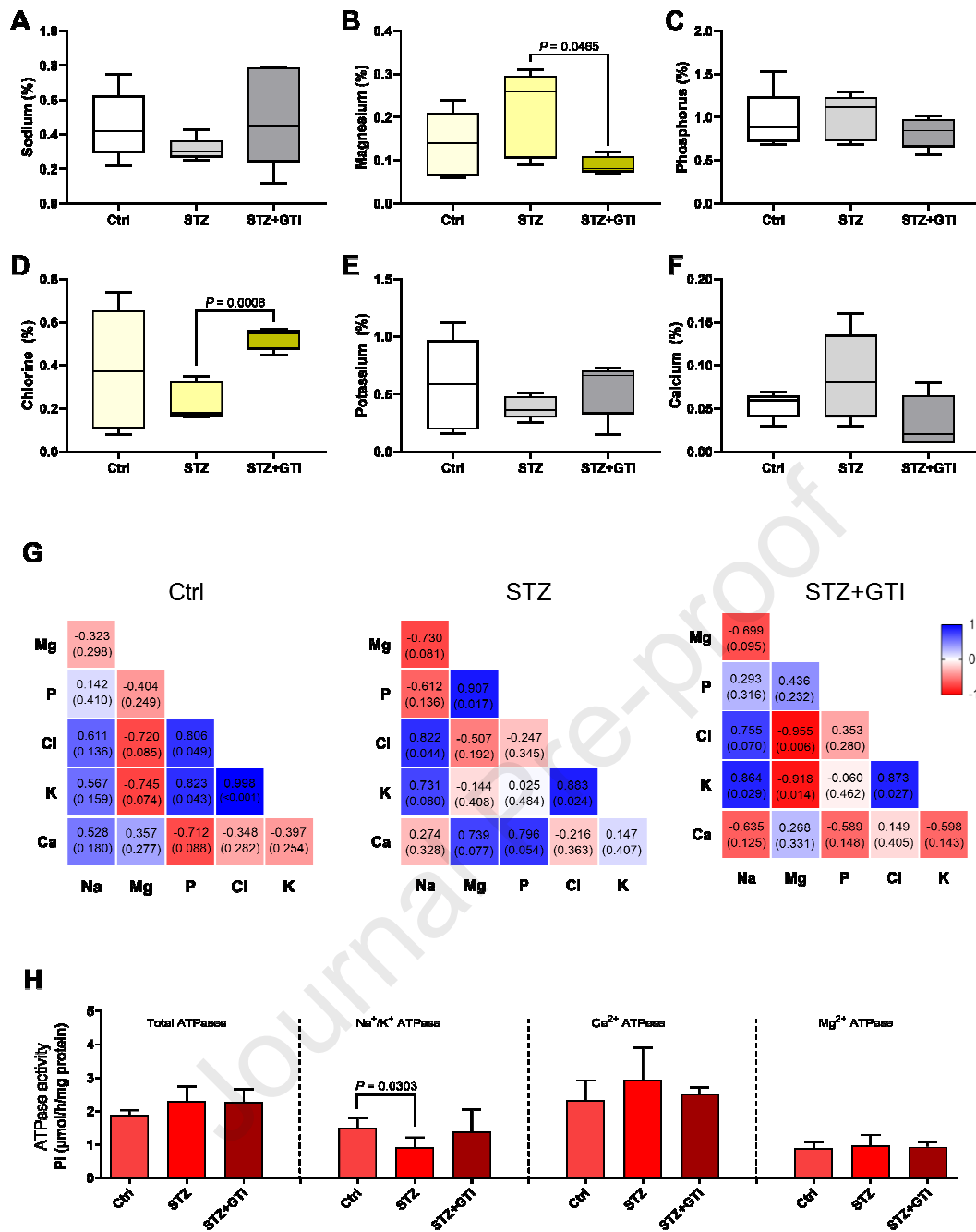


Figure 4

919

920

921

922

923

924

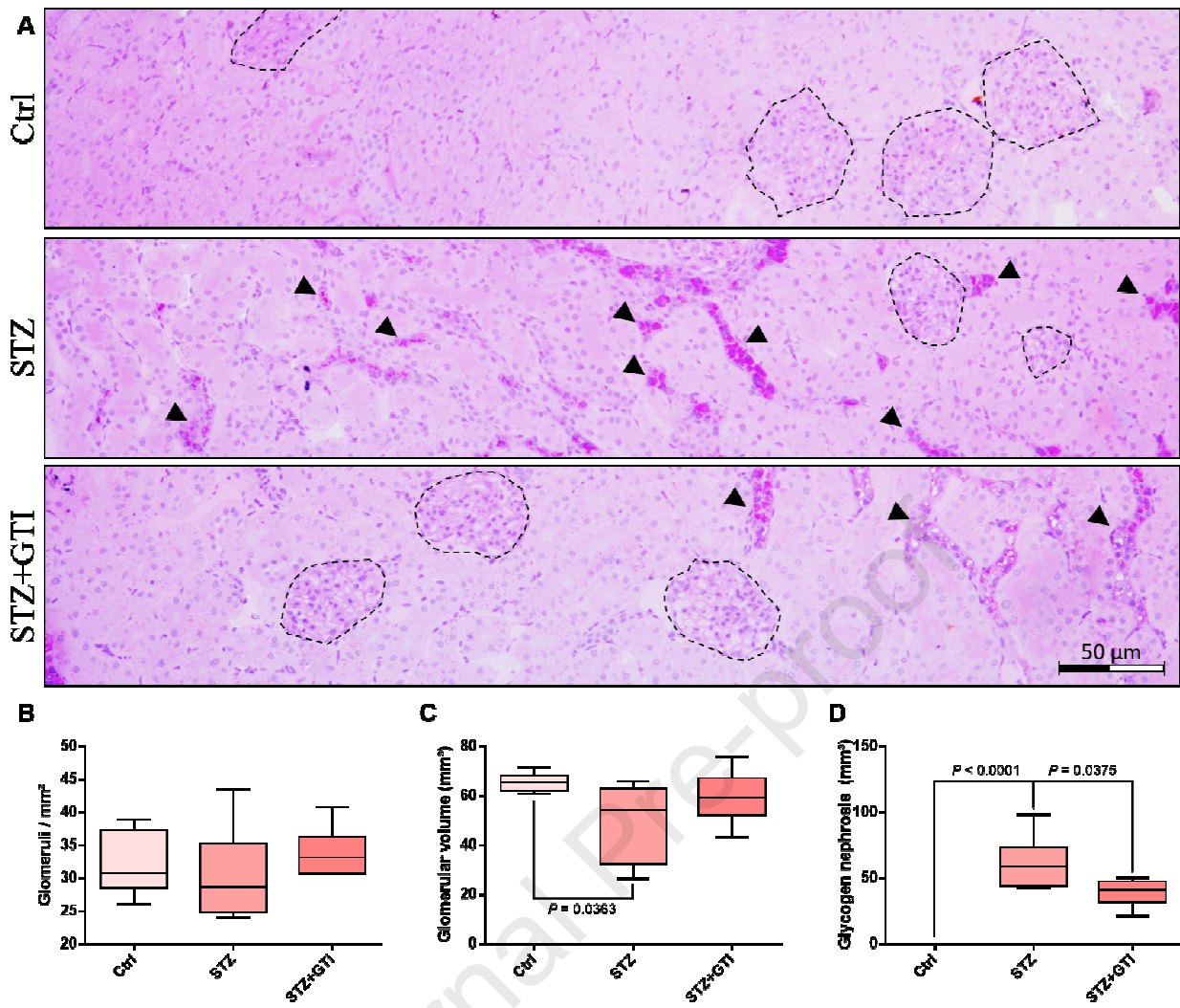


Figure 5

925

926

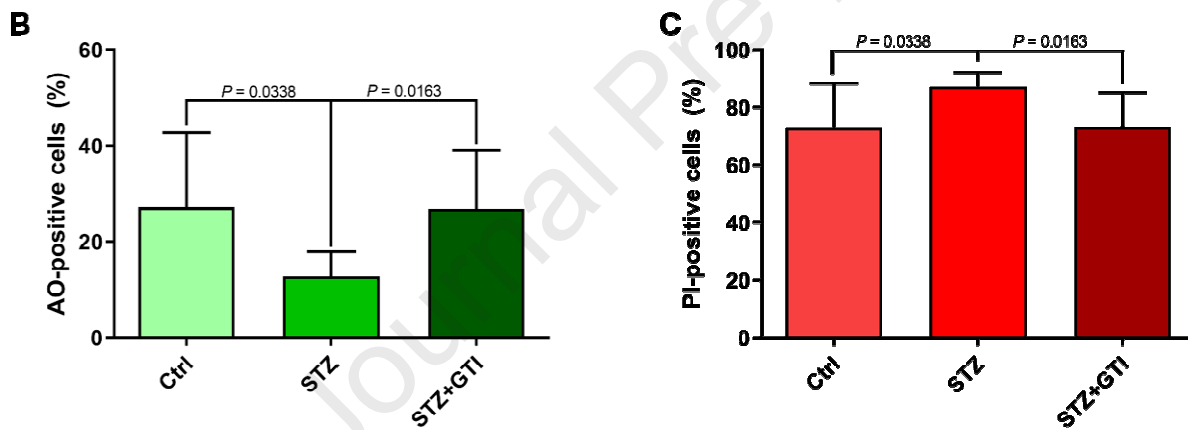
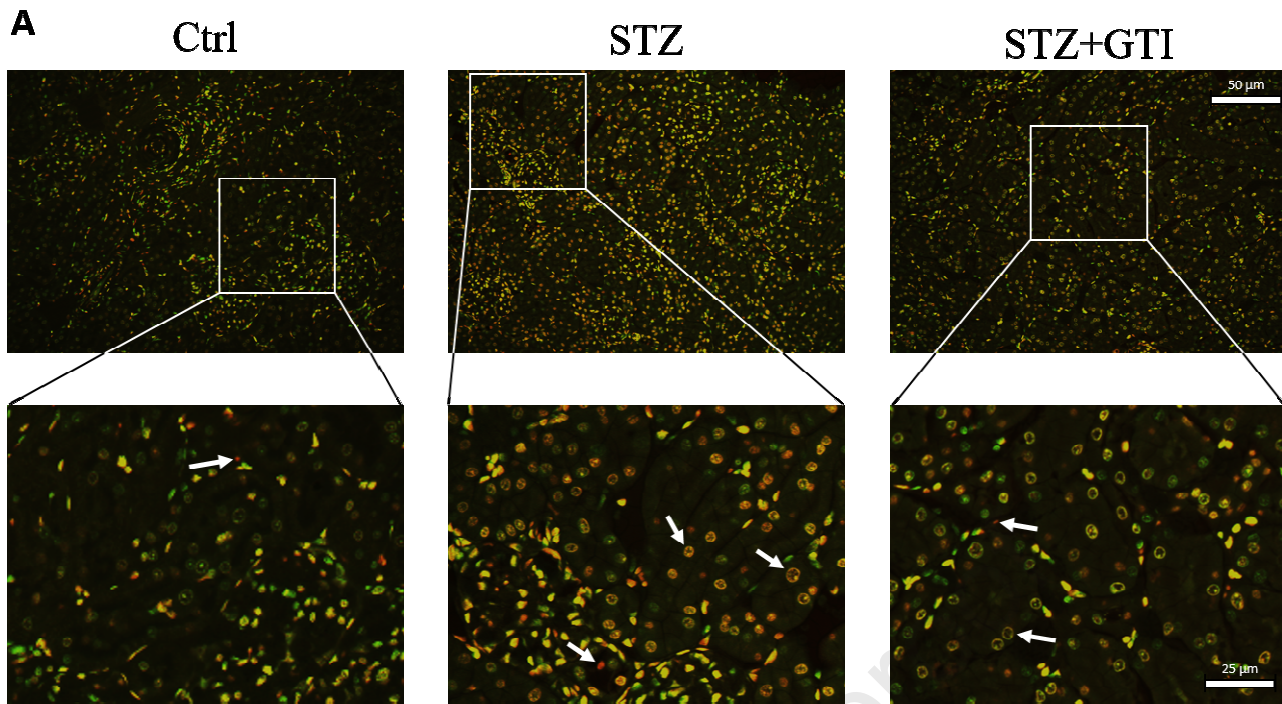
927

928

929

930

931



932

933

934

935

936

937

Figure 6

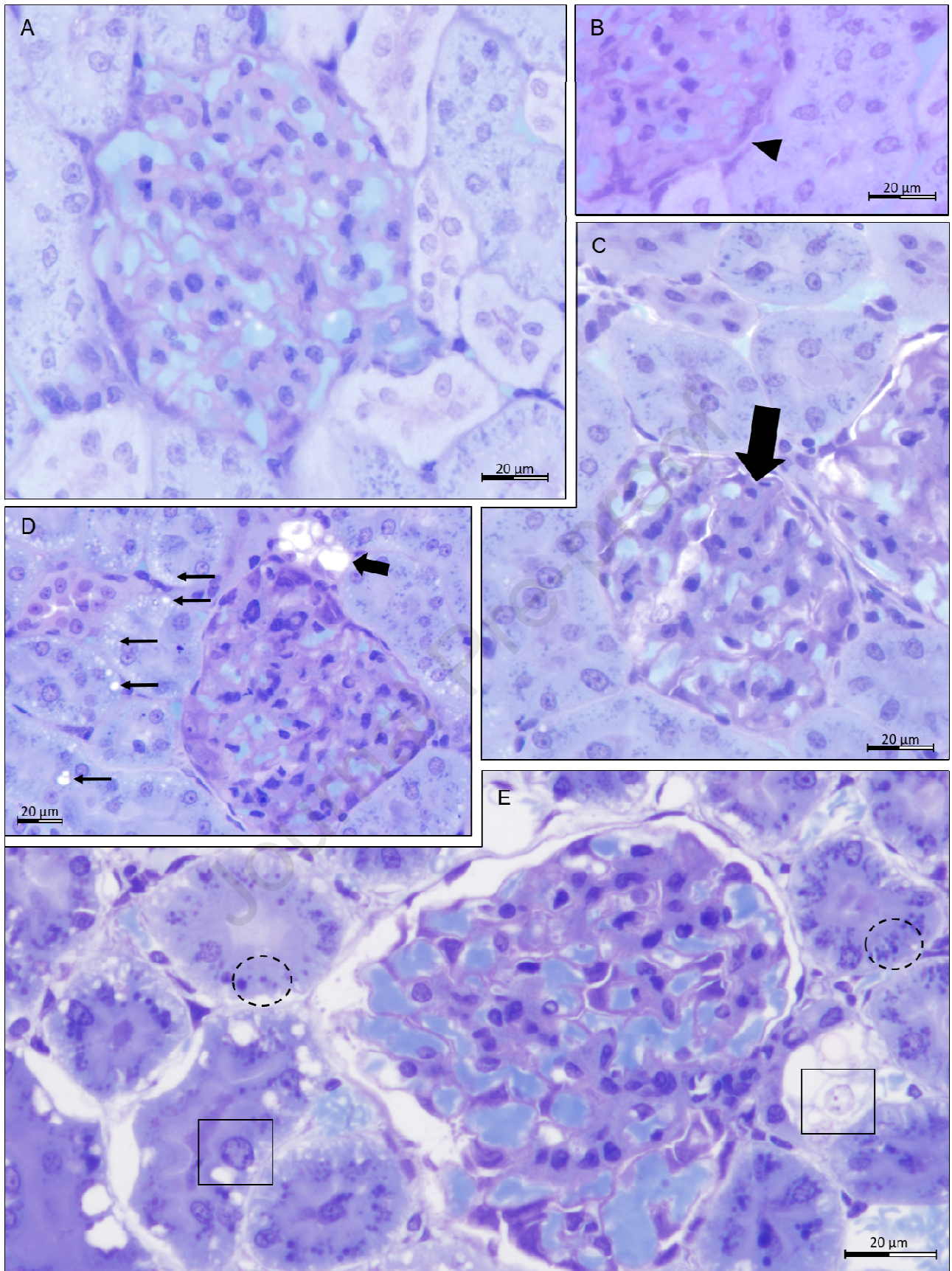
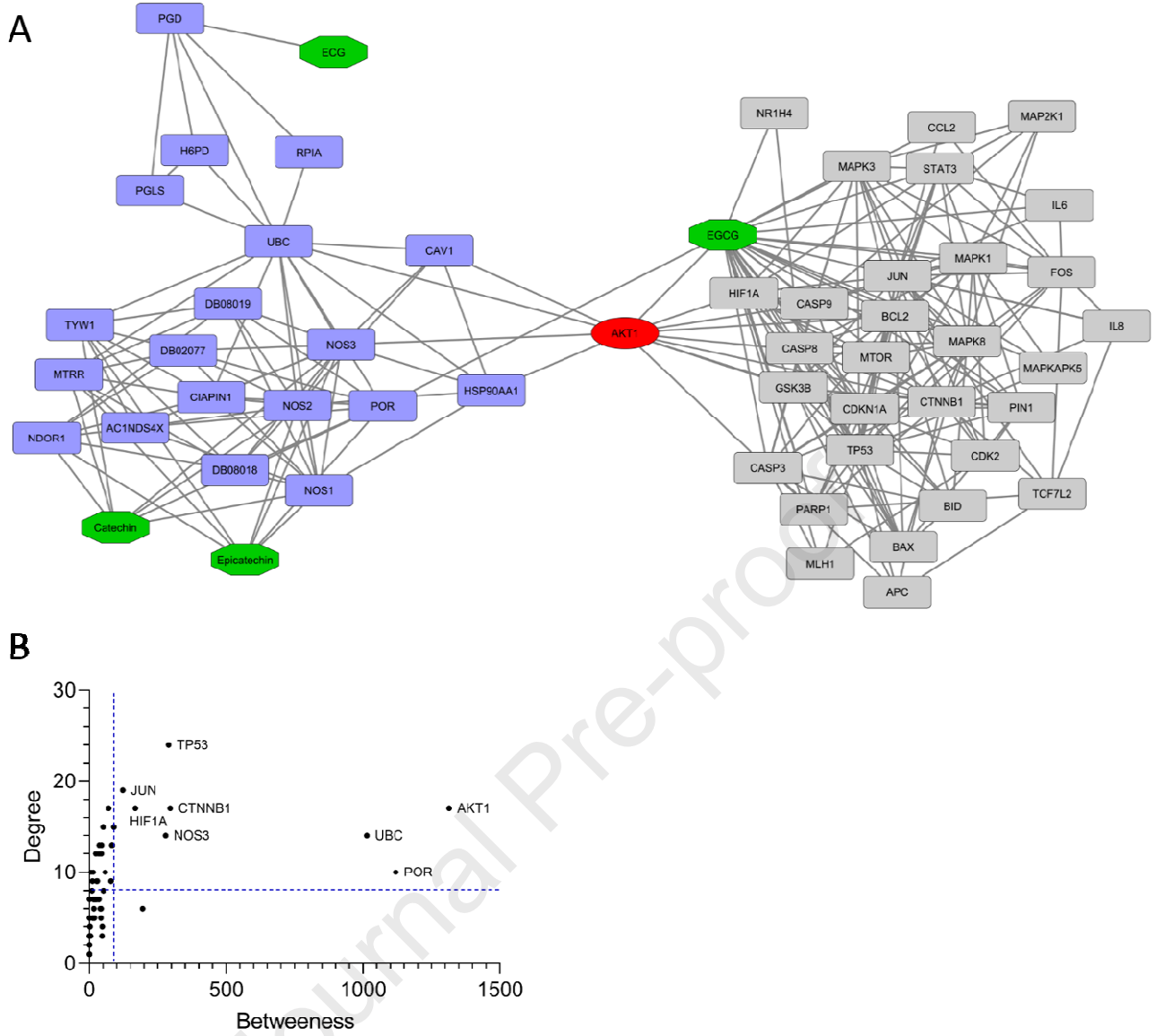


Figure 7

938  
939



**Figure 8**

940

941

942

943

944

945

946

947